UNIVERSITÀ DEGLI STUDI DI PADOVA

Dipartimento di Fisica e Astronomia "Galileo Galilei"

Corso di Laurea Magistrale in Fisica

Tesi di Laurea Magistrale

Functional integration methods for Rabi-coupled quantum gases

Relatore:

Prof. Luca Salasnich

Controrelatore:

Prof. Luca dell'Anna

Laureando:

Giovanni Francesco Bertacco

Anno Accademico 2017/2018

Thesis overview

The first chapter contains an introduction to the basic concepts of the physics of ultracold atoms. Primarily, we provide a historical background in which we present the theoretical and experimental main steps and deliverables in condensed matter physics that led to the modern approach to the study of ultracold quantum gases.
After having pointed out the important properties and issues of such systems, we propose a summary of the experimental techniques developed in these last thirty years, focusing on the gradual process of cooling at the nanoscale temperatures (laser cooling and evaporation) and Feshbach resonance.
The last part concerns the explanation of the concept of Rabi coupling: it consists in a linear coupling between the components of a quantum gas mixture, this means a tunneling between two internal hyperfine states by which one component can flip into the other.

In the second part of the thesis we investigate the properties of a multicomponent quantum Bose gas with a Rabi coupling, using theoretical methods based on functional integration.
Firstly, we derive the critical temperature of the gas with Rabi interaction but with the intra-species and inter-species coupling set to zero.
After that, we derive the mean field theory with non-zero interactions: the ground state solutions provide for two configurations, a symmetrical one and another with a population imbalance. We investigate the first case.
At very low temperatures beyond-mean-field contribution crucially affects the equation of state of many-body systems. We derive the equation of state of the gas including the quantum fluctuations. The divergent zero-point energy of gapless and

gapped elementary excitations of the uniform system is properly regularized obtaining a meaningful analytical expression for the beyond-mean-field equation of state in the weak Rabi coupling approximation.
In the case of attractive inter-particle interaction we show that the quantum pressure arising from Gaussian fluctuations can prevent the collapse of the mixture with the creation of a self- bound droplet. In particular we use a gaussian solution ansatz with appropriate parameters to investigate the stability and collective excitations of the droplet in the presence of the Rabi coupling.

In the third part we study the effects of Rabi coupling along the BCS-BEC crossover of a Feshbach resonance for a two-spin-component Fermi gas.
Results such as the gap equation, the number equation and the critical temperature in the mean-field approximation have been obtained. We find that the Rabi affects considerably the zero point energy of the fermions in BCS regime. As done for the bosonic case in chapter 2 we include quantum fluctuations to go further than the mean field solution.
We derive the gaussian contributes to the grand potential of the fermionic theory for the BCS-BEC crossover and subsequently we extend this result to the Rabi interacting case.

Contents

Chapter 1

Introduction

1.1 Historical background

What happens when a gas of atoms or molecules get colder and colder?
At very low temperatures quantum-mechanical properties of the matter becomes relevant: novel states appear and unseen phase transitions are observed. In such conditions we go deeper into the quantum degenerate regime where the quantum-statistical nature of the particles governs the dynamics.
The condensed matter physics provides the opportunity to discover new macroscopic quantum effects, no longer restricted to the subatomic world, but rather, determined by collective behavior of these many-body systems, to macroscopic scale.
Such systems have been an important challenge for an entire century, theoretically and experimentally, taking on issues of both fundamental and applied physics.

The theoretical prediction of Bose-Einstein-Condensation is one of the first steps towards the knowledge of superfluidity. Albert Einstein in 1924 studied the statistical properties of indistinguishable non-interacting bosons and he predicted the famous Bose-Einstein distribution [1]: a consequence of this BEC distribution is that below a certain critical temperature a macroscopic fraction of the particles occupies the same

quantum state.
In this case the solution of the fundamental problem preceded the related experiments on superfluidity of liquid helium, firstly discovered by Pyotr Kapitsa, John Allen and Don Misener in 1938 [2, 3].
The liquid can flow with null resistance and intriguing effects are observed such as quantized vortices and fountain effect. It is important to specify that the atoms in liquid helium are strongly interacting and they are far from the ideal case of non-interacting bosons.

The opposite case, in which the theory came after the experimental observations, is that of superconductivity, a phenomenon observed by Onnes in 1911 [4] and whom, only after an half of century, found his theoretical framework in the Bardeen-Schrieffer-Cooper theory [6]. A superconductor main characteristic is the Meissner effect [5]: below a certain critical temperature a perfect diamagnetism appears because any applied magnetic field is completely expelled from its interior.
This singular behaviour of these very cold metals can be explained considering electrons as a gas, where the electrons attract each others forming stable Cooper pairs.

Even after a century of studies and discoveries, condensed matter physics still has many interesting problems which require to be investigated.
For instance, in 1986, high-temperature superconductors were discovered in ceramic materials [7] and the precise microscopic mechanism governing these cuprates is still not clear today.
In the 90's, methods and techniques aimed to cooling and trapping atoms with lasers had been developed; together with the application of Feschbach resonance the interest towards the new physics of ultracold atoms considerably increased in the research community.

1.2 Ultracold atoms

In 1995 the first Bose-Einstein condensate has been experimentally obtained by Eric Cornell and Carl Wieman at NIST-JILA laboratories at Colorado University. Using laser cooling technology, they cooled atomic gas of rubidium to a temperature of about $6 \cdot 10^{-8}$ K. Cornell and Wieman, together with Wolfgang Ketterle, won the Nobel prize in 2001 ([8], [9], [10]). This discovery marked the birth of a new category of systems which can be succesfully isolated from the external enviroment and simultaneously accessibile for measure devices. Moreover, because of their complete isolation these ultracold gases are very clean in the sense that there are essentially no impurities unless deliberately added.

The main advantage of working with ultracold quantum gases is that interaction effects can be sufficiently small as to be treated with perturbation theory.
In order to have a dilute gas it is necessary to reach very low temperatures. These are impossible to achieve if the gas is in contact with material walls so the gas must be trapped into magnetic-optical traps after being cooled with laser beams. Once the atoms are trapped, evaporative cooling can be relatively easily implemented by lowering the trap depth, so that only the most energetic atoms can escape from the trap and the remaining gas cools after re-thermalization, in the same way as the common evaporation mechanism.

Another advantage of such systems is the flexibiliy: one can control the external trapping potential and the interatomic interaction through the Feschbach resonance. This allows for a systematic study of an enormous variety of interesting many-body systems, ranging from weakly interacting to strongly interacting, from one-dimensional to three-dimensional, from homogeneous to periodic, where the microscopic parameters are always precisely known and tunable.

1.2.1 Fano-Feschbach resonance

The Fano-Feshbach resonances (RFF) are important experimental techniques used to control properties of ultracold atoms such as the interaction strength of the coupling between particles.
Firstly, the resonances were applied in the context of nuclear physics and then they found crucial applications in ultracold atoms physics.
Such resonances have been predicted in 1995 [11] and firstly observed in a BEC of ^{23}Na [12]. Subsequently, Feshbach resonances for bosonic gas have been observed and this led to the realization of Bose-Einstein condensate of ^{85}Rb and causing it to collapse enhancing the strength of the interaction [13].
A fundamental achievement reached thanks to the Feshbach resonances is the production of ultracold molecules made of both bosons (^{85}Rb [14], ^{133}Cs [15, 16]) and fermions (^{40}K [17], ^{6}Li [18, 19, 20]).
It is important to notice that the molecules produced are bosons so it is possible to observe new phenomena related to a Bose-Einstein condensation of molecules made of fermionic atoms.
Observing such condensates raised the interest in the study of the evolution from the BEC regime to BCS regime (BEC-BCS crossover).

Let us consider two identical alkali atoms with an interaction $V_{bg}(r)$ which is a function of the relative distance, for simplicity it can be approximated to a Van der Waals potential. Taking into account the hyperfine structure, there is a coupling between electronic angular momentum and nuclear spin in addition to a possibile interaction of the total spin $\vec{F}$ of the atom with an external magnetic field.
Let us suppose that particles can be in two different channels, due to the splitting of the energy levels. If the kinetical energy of the atoms is lower than the energy separation of the two channels, we can make a distinction between a lower open channel and a closed forbidden one. A such condition can be obtained using ultracold alkali atoms. Turning on a magnetic field B we can remove the energy level degeneracy, forming sublevels quantized by F_z. Atoms can collide and doing a transition to the metastable state, so it is possible to increase and decrease the probability of the transitions.

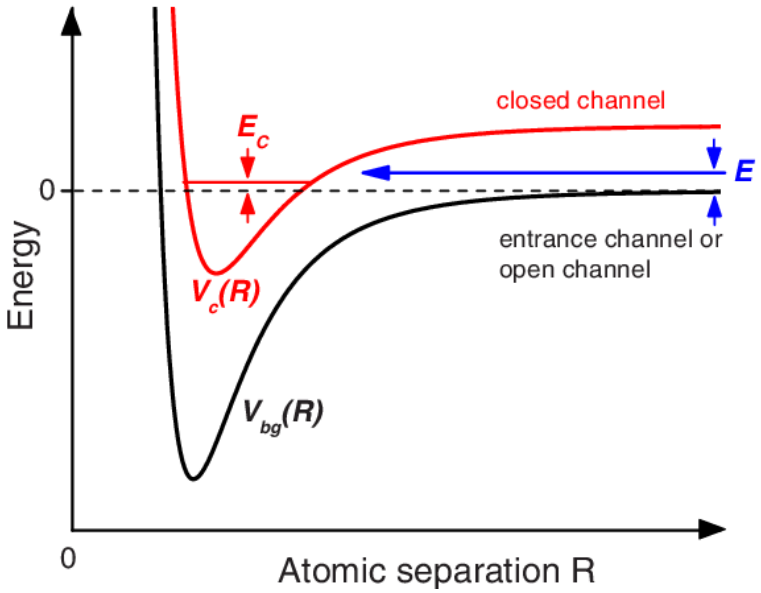

Figure 1.1: Fano-Feshbach resonance mechanism. The black line represents the open channel and the red line the closed one. With a magnetic field it is possible to allow a tunnelling between the two channels.

Tuning the magnetic field is possible to change the interaction between particles. An approximated relation is given by:

$$a = a_{bg}(1 - \frac{\Delta}{B - B_0}) \tag{1.1}$$

where a_{bg} is the background scattering length, Δ is a constant and B_0 is the value of the external magnetic field at resonance.

Let us notice that the scattering length can be both negative and positive: in the first case we have attraction while in the second we have repulsion.
It means that the Feschbach resonance allow us to vary the scattering length in a continuous way, passing through an intermediate phase in which the a diverges.
This limit is called unitarity.

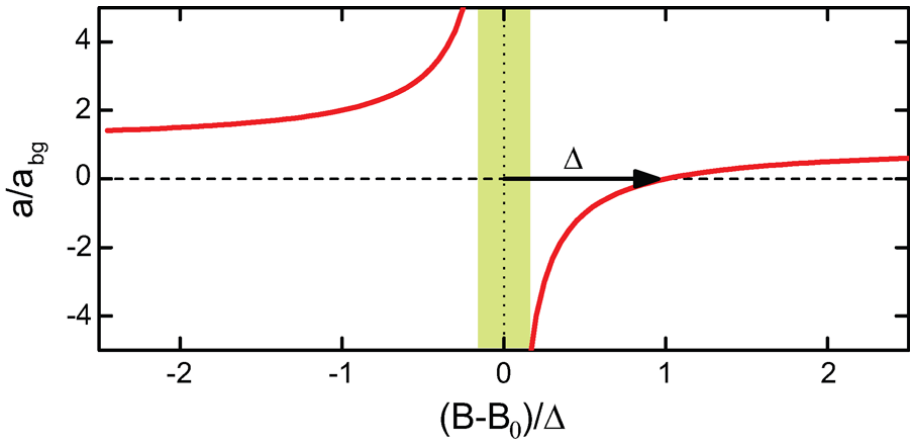

Figure 1.2: Scattering length as a function of the magnetic field. The costant Δ represent the resonance length. The unitary limit is at the resonant value B_0.

1.2.2 Experimental techniques

As stressed at the beginning of the chapter, the key issue in ultracold atoms physics is to obtain the diluteness condition. This is important for two reasons: the interaction between atoms is weak and it prevents liquefaction and solidification, furthermore only two-body interaction contributes to the dynamics, so this is a great advantage for the theoretical description. It is possible to prove that the degeneracy temperature is proportional to $n^{2/3}$ where n is the density of particles. Due to this, the cooling must be of the order of nanokelvin.

Firstly, it is necessary to create conditions to make thermal insulation, so the gas is introduced into a vacuum chamber and then trapped by using magnetic-optical traps (MOT). Using an MOT we can generate a restoring force space-dependent headed to an origin point. The experimental set-up used for the confinement consists of two circular coils in anti-Helmoltz configuration and two counter-propagating lasers with opposite polarization σ_- and σ_+.

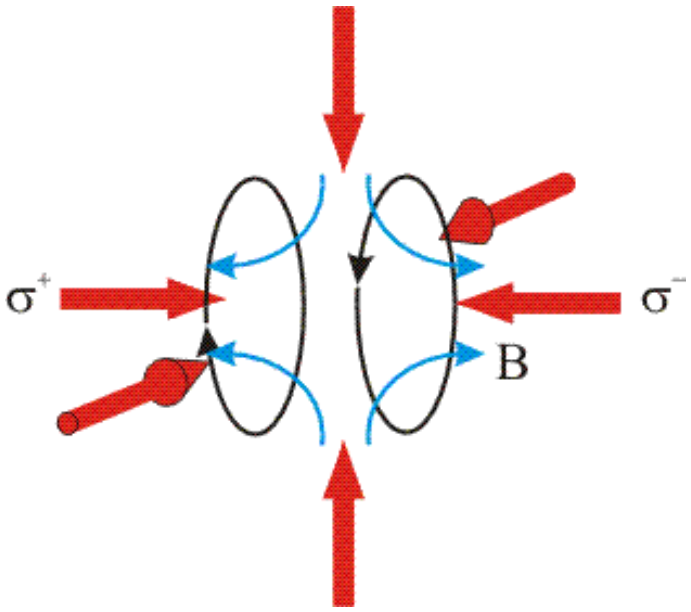

Figure 1.3: 3-D magnetic-optical trap. The beams are set in an orthogonal configuration to provide the confinement

The coils generate a linear magnetic field along the confinement axes, it is null at the origin and it increases moving away from it. By exploiting the hyperfine structures of the atoms and the Zeeman coupling between the magnetic field and the total spin of the atom we can generate a force headed to origin due to the pressure of the magnetic beams with positive and negative polarization.

Once the gas is confined by magnetic-optical trap it is possible to decrease the temperature using laser cooling.
Let us consider an electromagnetic wave which interacts with an atom with a frequency slightly lower than a specific frequency of an atomic transition from the ground state to an excited state. Due to this slight detuning and the Doppler effect caused by the kinetic energy of the particles, a fraction of the atoms decelerates and the transition takes place.
After that, the excited atom spontaneously emits in an isotropically configuration: the overall effect is a decreasing of average velocity caused by the laser beams.

So, once the gas is confined with an MOT it is sufficient to use a set of three orthogonal counter-propagating laser beams with a slight detuning at resonance to cool the atoms

to a certain limit temperature due to the Heisemberg principle, of about a hundred of μK.

To go beyond this limit we need to use forced evaporation. It consists of removing the most energetic particles of the gas and, after this, in rethermalization of the remaining atoms.
Inside the trap the atoms follow a certain distribution of energies: using particular electromagnetic beams at radiofrequency we can stimulate the outflow of the most energetic particles from the trap.
The overall effect is a decreasing of the total energy of the system, with a consequent nanoscale cooling.

Once we have done that, the system must relax to equilibrium configuration. It can be done through the particle collisions. For fermionic gases this is a problem, in fact because of the Pauli exclusion principle the s-wave scattering process is fully inhibited and it cannot thermalize. For this reason, treating the fermions with sympathetic cooling we can solve the problem: inside the fermion gas we insert a boson gas which acts as coolant.

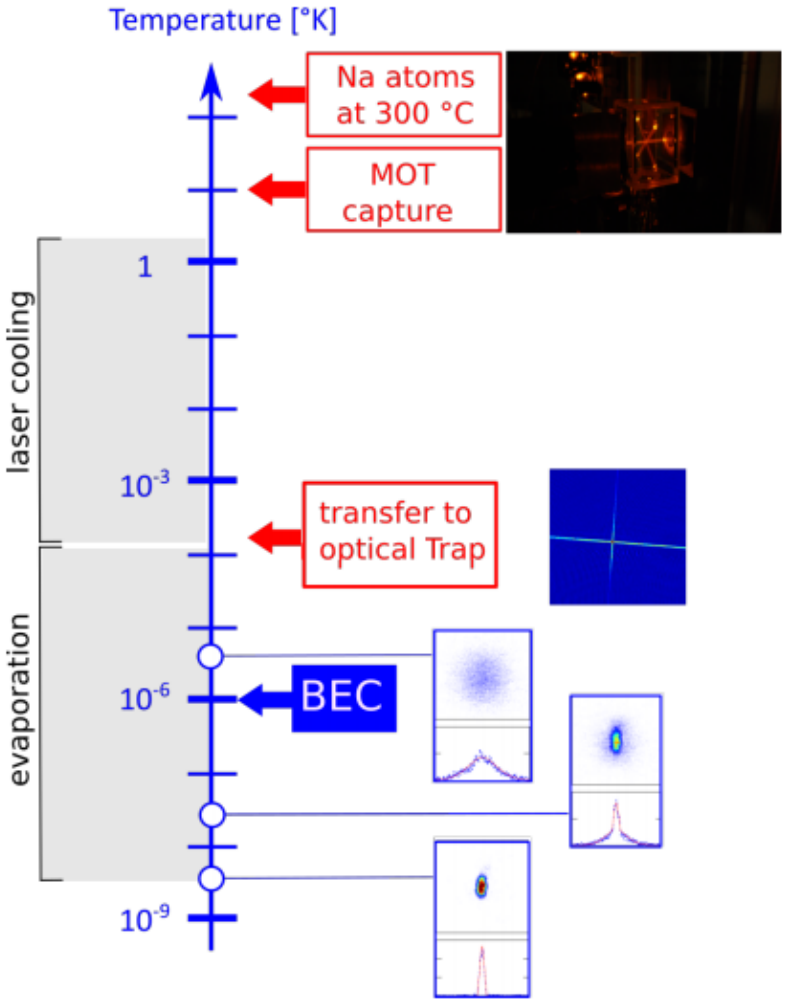

Figure 1.4: Gradual process of cooling at nanoscale temperature for atomic quantum gases. Laser cooling technique can bring the system to temperatures of μK. After evaporation the system can be cooled at the desired nanoscale level.

1.3 Rabi coupling

The phase coherence on macroscopic scales is a quantum-mechanical property of a weakly interacting Bose-Einstein condensate and it is a spectacular phenomenon occurring in superfluids and superconductors. It is obviously impossible to measure the phase of a condensate, but if we take into account more BECs we can evaluate the relative phases. The most important example is the dynamical evolution of two coupled macroscopic quantum systems in the Josephson-junction experiment, in which a superconducting current of Cooper pairs exhibits coherent oscillations. The Josephson effect has been predicted in the sixties [21], and has been verified experimentally in 1982 [22]. An analogous example on a BEC of dilute atomic gases can be found in [23]. Preparing two initially isolated condensates in a double-well potential, made it dividing a harmonic magnetic trap in two halves using a laser beam and then lowering the central barrier, we can form a coupling between the two different BECs. One can then observe the time rate of change of the relative population caused by the tunneling, which is the analogous quantity to the current of Cooper pairs in the usual Josephson experiments. However, many experimental difficulties are associated with the stability and the spatial dimensions of the laser beam make this task difficult.
A more successful technique to observe Josephson oscillations is to consider two different internal hyperfine states: in this case the current is between different spin states. The Josephson effect was put on its theoretical foothold by Leggett in 1999 who defines it as *the dynamics of N bosons restricted to occupy the same two-dimensional single particle Hilbert space*. Leggett introduced three regimes where they differ from one to another in different relationships between tunnelling (linear coupling between condensates) and interaction (self-particle quartic terms): non-interacting Rabi regime, weakly interacting Josephson regime and strongly interacting Fock regime. A Rabi term can be induced by microwave or radio-frequency techniques, or by two-photon Raman transitions induced by two opportunely detuned laser beams [24, 25]. In the second quantization framework, it is related to the destruction of a component followed by the creation of another. The introduction of this sort of oscillation enriches the physics of quantum gas binary mixtures both experimentally and theoretically.

Chapter 2

Two component Rabi-coupled Bose gas

In this section we adopt a functional integration framework to deeply investigate the properties of a two component Rabi-coupled Bose gas.
In the first place we introduce an Euclidian action $S[\Psi, \bar{\Psi}]$ of the bosonic fields in order to write the partition function Z of the system summing up over the two dimensional complex field associated to the mixture of bosons.
Firstly, in absence of any interactions, but with the Rabi-coupling, we derive the critical temperature for the superfluid. The knowledge of the partition function (total or partial in specific degrees of approximation) allow us to calculate the grand potential in function of the temperature, chemical potential and volume. The thermodynamic properties of our gas are so obtained taking derivatives of the potential.
In particular we are interested in the equation of state of the system. We start from a mean field point of view for the bosonic fields, this time with non-zero interaction intra- and inter-species; then we include the quantum fluctuations using a Bogoliubov transform through a gaussian integration of the excitation field over the ground state. In this framework, we reproduce the energy spectrum as poles of the Bogoliubov propagator already found by Abad M. and Recati A. in 2003 [31] and we derive the grand potential as a sum of a mean field contribution and a gaussian fluctuations

contribution, highlighting how the quantum excitations affect the equation of state. From here on out we adopt the following convention: $k_B = 1$, $\hbar = 1$, $m = 1$.

2.1 Non-interacting theory

Firstly, we consider the case of a coherent system made of two component bosons with Rabi interaction between the two hyperfine states of the quantum gas, with no other interactions. Each component acts like an independent free Bose gas except for the presence of the the Rabi oscillations: a state can turn into another, the overall result is that the system has the same behaviour of a mixture of two component free gas, one with $\mu_a = \mu + \omega_R$ and the second $\mu_b = \mu - \omega_R$.

The euclidean action reads:

$$S_0[\Psi, \bar{\Psi}] = \int_0^\beta d\tau \int d^3x \; \Psi_a^*[\partial_\tau - \frac{1}{2}\nabla^2 - \mu]\Psi_a + \Psi_b^*[\partial_\tau - \frac{1}{2}\nabla^2 - \mu]\Psi_b + \Psi_b^*\omega_R\Psi_a + \Psi_a^*\omega_R\Psi_b. \tag{2.1}$$

In the absence of interactions the last formula can be written as a quadratic form. The exact partition function is then:

$$Z = \int D[\Psi, \bar{\Psi}] e^{-\bar{\Psi}\hat{G}_{\omega_R}\Psi} \tag{2.2}$$

where $\Psi = \binom{\Psi_a}{\Psi_b}$ and

$$G^{-1}_{\omega_R}(k) = \begin{bmatrix} -i\omega_n - \varepsilon(\vec{k}) & -\omega_R \\ -\omega_R & -i\omega_n + \varepsilon(\vec{k}) \end{bmatrix} \tag{2.3}$$

with $\varepsilon(\vec{k}) = \frac{k^2}{2} - \mu$.

The partition function can be calculated using gaussian integrals. The calculations

for the grand potential is straightforward:

$$\Omega_{\omega_R} = -\frac{1}{\beta}\log(Z) = \frac{1}{\beta}\sum_{\vec{k},i\omega_n}\log(\lambda_1\lambda_2) = \Omega_0(\mu+\omega_R) + \Omega_0(\mu-\omega_R) \tag{2.4}$$

where Ω_0 is the non-interacting single component grand potential and λ_1 and λ_2 are the eigenvalues of the inverse of the propagator.

$$\begin{aligned}\lambda_1 &= -i\omega_n + \frac{k^2}{2} - (\mu+\omega_R)\\ \lambda_2 &= -i\omega_n + \frac{k^2}{2} - (\mu-\omega_R).\end{aligned} \tag{2.5}$$

2.1.1 Critical temperature

In the special case of the non-interacting gas we are able to give the exact expression for the grand potential in presence of Rabi-coupling.
From this result it is possible to derive the thermodynamic relations for the gas. In this section we are interested in the critical temperature.
Our intention is to take the density of particles and to search for the conditions under which we have a macroscopic occupation of the ground state in this particular quantum system [32-33].

Taking the derivative of the thermodynamic potential

$$N = -\frac{\partial\Omega_{\omega_R}}{\partial\mu} = \sum_{\vec{k}}\frac{1}{e^{\beta(\frac{k^2}{2}-(\mu+\omega_R))}-1} + \frac{1}{e^{\beta(\frac{k^2}{2}-(\mu-\omega_R))}-1}. \tag{2.6}$$

In 3-D, in the continuous limit $\sum_{\vec{k}} \to L^3\int d^3k/(2\pi)^3$:

$$n = (\frac{T}{2\pi})^{\frac{3}{2}}[f(e^{\beta(\mu+\omega_R)}) + f(e^{\beta(\mu-\omega_R)})] \tag{2.7}$$

where the function $f(z)$ is defined as:

$$f(z) = \sum_{n=1}^{\infty} \frac{z^n}{n^{\frac{3}{2}}}. \tag{2.8}$$

The convergence radius of the series is $|z| < 1$.
This condition limits the domain of the chemical potential:

$$\begin{aligned} \mu - \omega_R &< 0 \\ \mu + \omega_R &< 0. \end{aligned} \tag{2.9}$$

Since the Rabi parameter is positive we have an upper limit for the chemical potential: $\mu < -\omega_R$.
Therefore, we expect that, fixing the number of particle n, the critical temperature is given inverting the following formula:

$$n = (\frac{T_{c,\omega_R}}{2\pi})^{\frac{3}{2}}[\zeta(3/2) + f(e^{\frac{-2\omega_R}{T_{c,\omega_R}}})]. \tag{2.10}$$

From the last result we can deduce how the critical temperature for a system Rabi-coupled (T_{c,ω_R}) is always lower than the free theory case (T_c).

In fact, after simple calculations:

$$\frac{T_{c,\omega_R}}{T_c} = [\frac{1}{1 + f(e^{\frac{-2\omega_R}{T_{c,\omega_R}}})}]^{\frac{2}{3}} \tag{2.11}$$

and the function f is always positive since

$$0 < f(e^{\frac{-2\omega_R}{T_{c,\omega_R}}}) < \zeta(\frac{3}{2}). \tag{2.12}$$

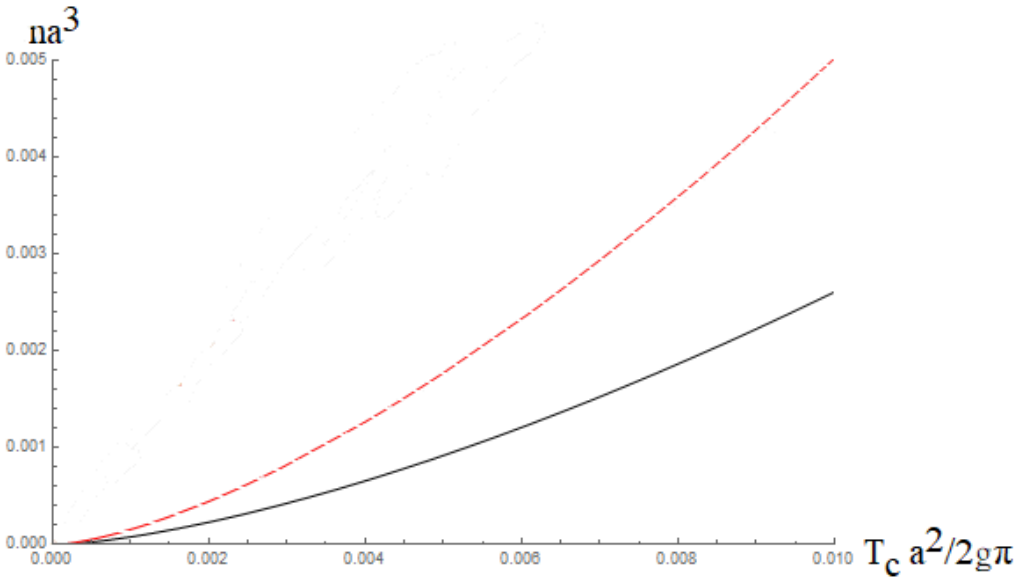

Figure 2.1: Plot of the rescaled version of equation (2.10). Black solid line represents the Rabi-less case while in the red-dashed line we set the Rabi coupling to $a^2\omega_R/2\pi = 0.1$. At fixed number density the presence of the Rabi decreases the critical temperature.

2.2 Interacting two component Rabi-coupled Bose gas

2.2.1 Mean field approximation

We start from a Path Integral approach.
The action of the theory is:

$$\begin{aligned} S[\Psi,\bar{\Psi}] = \int_0^\beta d\tau \int d^3dx\ \Psi_a^*[\partial_\tau - \frac{1}{2}\nabla^2 - \mu]\Psi_a + \Psi_b^*[\partial_\tau - \frac{1}{2}\nabla^2 - \mu]\Psi_b \\ + \frac{1}{2}g_a\left|\Psi_a\right|^4 + \frac{1}{2}g_b\left|\Psi_b\right|^4 + g_{ab}\left|\Psi_a\right|^2\left|\Psi_b\right|^2 + \Psi_b^*\omega_R\Psi_a + \Psi_a^*\omega_R\Psi_b. \end{aligned} \tag{2.13}$$

The partition function is defined as:

$$Z = \int D[\Psi,\Psi^*]e^{-S[\Psi,\Psi^*]}. \tag{2.14}$$

The presence of the Rabi coupling in the Euclidean action in equation (2.13) implies that only the total number of atoms is conserved, so we use a unique chemical potential.

The central point of the mean field approximation is to assume a stationary and homogeneus configuration for the bosonic fields:

$$\begin{aligned} \Psi_a(\vec{x},\tau) &= \nu_a \\ \Psi_b(\vec{x},\tau) &= \nu_b, \end{aligned} \tag{2.15}$$

Inserting (2.15) in (2.13) we find the mean field grand potential

$$\frac{\Omega_0}{L^3} = -\mu\nu_a^2 + \frac{1}{2}g_a^4 - \mu\nu_b^2 + \frac{1}{2}g_b^4 + g_{ab}\nu_a^2\nu_b^2 - 2\omega_R\nu_a\nu_b, \tag{2.16}$$

We notice that the order parameters ν_a and ν_b must satisfy the minimum criteria:

$$\begin{aligned}\mu\nu_a &= (g_a\nu_a^2 + g_{ab}\nu_b^2)\nu_a - \omega_R\nu_b \\ \mu\nu_b &= (g_b\nu_a^2 + g_{ab}\nu_a^2)\nu_b - \omega_R\nu_a.\end{aligned} \tag{2.17}$$

For simplicity from now on we consider the case $g = g_a = g_b$. As we will explain later, this condition is straightforward achievable experimentally.
Rewriting equation (2.17) we get that the equilibrium configuration must satisfy

$$[g - g_{ab} + \frac{\omega_R}{\nu_a\nu_b}](\nu_a^2 - \nu_b^2) = 0. \tag{2.18}$$

At this point there are two possibilities for the ground state,
naming $\Delta = \nu_a^2 - \nu_b^2$:

$$\begin{aligned}&Symmetric \quad \Delta = 0 \\ &Polarized \quad \Delta = \pm n\sqrt{1 - (\frac{2\omega_R}{n(g - g_{ab})})^2}\end{aligned} \tag{2.19}$$

where $n = \nu_a^2 + \nu_b^2$.

For the purpose of having a complete description of the mean field gas it is necessary to impose the stability of the ground state taking the Hessian matrix of the grand potential and imposing it to be positive.
After calculating the eigenvalues of the matrix $\frac{\partial^2\Omega_0}{\partial\nu_b\partial\nu_a}$ we get the following stability conditions [31, 38-40]:

$$g + g_{ab} > 0 \tag{2.20}$$

$$g - g_{ab} + 2\frac{\omega_R}{n} > 0. \tag{2.21}$$

Before getting to the bottom of the issue of the ground state stability, we need to point out that the intra-species interaction must be repulsive and the inter-species interaction must be attractive. In fact, considering the opposite case, it is clear that the gas evolves in a phase separation configuration, of course of very little interest.

Before we go any further, we must consider the relation between n and the chemical potential μ.

From (2.17) we get:

$$\begin{aligned} &Symmetric \quad n = 2\frac{\mu + \omega_R}{g + g_{ab}} \\ &Polarized \quad n = \frac{\mu}{g}. \end{aligned} \tag{2.22}$$

Using (2.20) and (2.21) we find the following phase diagram:

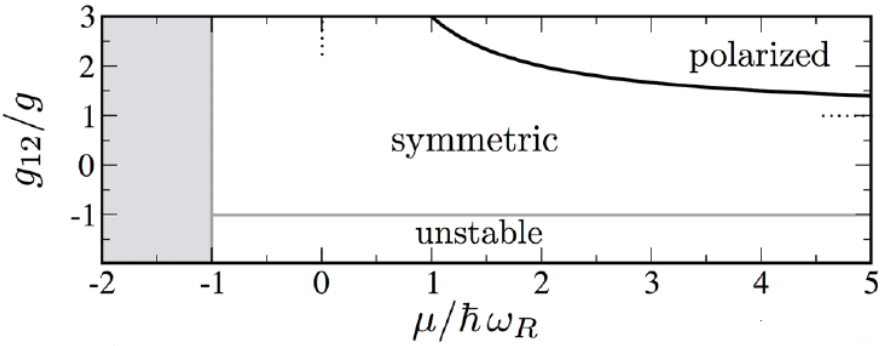

Figure 2.2: Phase diagram for the mean-field configuration. In the symmetric ground state the two components appear with the same particle density, whereas in the polarized phase densities are unequal. For $\frac{g_{12}}{g}$<-1 the symmetric solution is unstable in the thermodynamic limit. The grey region represents the trivial solution $n = 0$.

In the symmetric ground state case the mean field grand potential reads as:

$$\frac{\Omega_0}{L^3} = -\frac{(\mu + \omega_R)^2}{(g + g_{ab})}. \tag{2.23}$$

It is immediate to get the energy density of the system from equations (2.22) and (2.23) in the mean field approximation, since $\xi_0 = \frac{E_0}{L^3} = \frac{\Omega_0}{L^3} + n\mu$ where $n = -\frac{\Omega_0}{\partial\mu}$.
In dimensionless units we finally obtain:

$$\frac{\mathcal{E}}{E_B/a^3} = \pi(1 + \eta)\bar{n}^2 - \bar{\omega_R}\bar{n} \tag{2.24}$$

where $\bar{n} = na^3$ is the diluteness parameter, $\eta = \frac{g}{g_{ab}}$, $E_B = \frac{1}{a^2}$ is the energy unit and $\bar{\omega}_R = \frac{\omega_R}{E_B}$.

At this point it is necessary to make a few remarks on the stability of the system in the mean field configuration.
As we can see from equation (2.24) the energy present a minimun only if $\eta > -1$, according with equation (2.20). Anyway we have another stability condition given by equation (2.21), rewriting it as $\eta < 1 + 2\frac{\omega_R}{n}$ we conclude that for $\eta > 1$ we have instability at the thermodynamic limit.

We calculated the equation of state in the mean field approximation, in the next section we consider important contributions that can be added to the formula. These kind of contributions are related to quantum and thermal fluctuations, so we need to go beyond the mean field. The following discussion is based on the symmetric ground state condition.

2.2.2 Quantum fluctuations

Let us consider the action of the Rabi-coupled Bose mixture in equation (2.13)

$$S[\Psi, \bar{\Psi}] = \int_0^\beta d\tau \int d^3x \; \Psi_a^*[\partial_\tau - \frac{1}{2}\nabla^2 - \mu]\Psi_a + \Psi_b^*[\partial_\tau - \frac{1}{2}\nabla^2 - \mu]\Psi_b$$
$$+\frac{1}{2}g_a \left|\Psi_a\right|^4 + \frac{1}{2}g_b \left|\Psi_b\right|^4 + g_{ab} \left|\Psi_a\right|^2 \left|\Psi_b\right|^2 + \Psi_b^*\omega_R\Psi_a + \Psi_a^*\omega_R\Psi_b.$$

In the previous section we used the static and homogeneous field ansazt to calculate the partition function at the mean field level of approximation. The idea is to go further including the dynamics of collective excitation through the so-called Bogoliubov transformation. Our purpose is to shift the parameters, which represent the mean field static and homogeneus solution, with a small perturbation space and time dependent. Taking into account in the action (2.13) only the quadratic terms in the Bogoliubov new fields, neglecting higher order terms we can calculate the partition

function performing gaussian integration.

$$\begin{aligned}\Psi_a &= \nu_a + \eta_a(\tau, \vec{x}) \\ \Psi_b &= \nu_b + \eta_b(\tau, \vec{x}).\end{aligned} \tag{2.25}$$

So, inserting (2.25) in equation (2.13), calling $\eta = (\eta_a, \eta_b)^T$ [34-36] we use the saddle point condition given by (2.17). We therefore consider a symmetric ground state condition $\nu = \nu_a = \nu_b$.

Finally we perform the Fourier transform to get the quadratic form:

$$S^{(2)}[\eta, \bar{\eta}] = \frac{1}{2} \sum_{i\omega_n, \vec{k}} \bar{\eta}(i\omega_n, \vec{k}) \mathbb{M}(i\omega_n, \vec{k}) \eta(i\omega_n, \vec{k}). \tag{2.26}$$

The matrix $\mathbb{M}$ represents the inverse of the fluctuations propagator:

$$\mathbb{M}(i\omega_n, \vec{k}) = \begin{bmatrix} \mathbb{M}_{11} & \mathbb{M}_{12} & \mathbb{M}_{13} & \mathbb{M}_{14} \\ \mathbb{M}_{12} & \mathbb{M}_{22} & \mathbb{M}_{14} & \mathbb{M}_{13} \\ \mathbb{M}_{13} & \mathbb{M}_{14} & \mathbb{M}_{11} & \mathbb{M}_{12} \\ \mathbb{M}_{14} & \mathbb{M}_{13} & \mathbb{M}_{12} & \mathbb{M}_{22} \end{bmatrix} \tag{2.27}$$

where

$$\begin{aligned}\mathbb{M}_{11}(k) &= \frac{1}{\beta L^3}(i\omega_n - \vec{k}^2 + \mu - g\nu^2 - \frac{g_{12}}{2}\nu^2) \\ \mathbb{M}_{22}(k) &= \frac{1}{\beta L^3}(-i\omega_n - \vec{k}^2 + \mu - g\nu^2 - \frac{g_{12}}{2}\nu^2) \\ \mathbb{M}_{12}(k) &= -\frac{1}{\beta L^3}\frac{g\nu}{\sqrt{2}} \\ \mathbb{M}_{13}(k) &= \frac{1}{\beta L^3}(\omega_R - g_{12}\frac{\nu^2}{2}) \\ \mathbb{M}_{14}(k) &= -\frac{1}{\beta L^3}\frac{g_{12}\nu^2}{2}\end{aligned} \tag{2.28}$$

Diagonalizing $\mathbb{M}_{14}(0,\vec{k})$ we obtain the spectrum of elemetary excitations:

$$\begin{cases} E_1(\vec{k}) = \sqrt{\frac{\vec{k}^2}{2}(\frac{\vec{k}^2}{2} + 2(\mu + \omega_R))} \\ \\ E_2(\vec{k}) = \sqrt{\frac{\vec{k}^2}{2}(\frac{\vec{k}^2}{2} + A(\mu,\omega_R)) + B(\mu,\omega_R)} \end{cases} \tag{2.29}$$

where

$$A(\mu,\omega_R) = (\mu + \omega_R)(\frac{1-\eta}{1+\eta}) + 2\omega_R \tag{2.30}$$

and

$$B(\mu,\omega_R) = 4\omega_R((\mu + \omega_R)(\frac{1-\eta}{1+\eta}) + \omega_R). \tag{2.31}$$

We remind that $\eta = \frac{g}{g_{ab}}$.

At this point we are able to write the grand potential as a sum of a mean field term plus a gaussian contribution [36-41]:

$$\Omega = \Omega_0 + \frac{1}{2\beta}\sum_{i\omega_n,\vec{k}} \log\det \mathbb{M}(i\omega_n,\vec{k}). \tag{2.32}$$

We are not interested in thermal fluctuations, so we take the zero temperature approximation.
The grand potential is then the sum of a mean field term Ω_0 and a zero point energy term Ω_g:

$$\Omega_g(\mu) = \frac{1}{2}\sum_{\vec{k}}[E_1(\vec{k},\mu) + E_2(\vec{k},\mu)]. \tag{2.33}$$

The chemical potential must be fixed using the ground state symmetric saddle point condition $n = 2\frac{\mu+\omega_R}{g+g_{ab}}$, so

$$\begin{cases} E_1(\vec{k}) = \sqrt{\frac{\hbar^2\vec{k}^2}{2m}(\frac{\vec{k}^2}{2m} + (g+g_{ab})n)} \\ \\ E_2(\vec{k}) = \sqrt{\frac{\hbar^2\vec{k}^2}{2m}(\frac{\vec{k}^2}{2m} + (g-g_{ab})n + 4\omega_R) + 2\omega_R(g-g_{12})n + 2\omega_R}. \end{cases} \tag{2.34}$$

In the continuum limit $\sum_{\vec{k}} \to L^3 \int d^3k/(2\pi)^3$ the quantum fluctuations reads:

$$\Omega_g^0 = \frac{1}{4\pi^2}\int_0^\infty dq E_1(q) + \frac{1}{4\pi^2}\int_0^\infty dq E_2(q). \tag{2.35}$$

The first ungapped term is similar to the interacting Rabi-less case discussed in reference [42], after regularization [44] we get:

$$\frac{1}{4\pi^2}\int_0^\infty dq E_1(q) = \frac{8}{15\pi^2}(\mu + \hbar\omega_R)^{\frac{5}{2}}. \tag{2.36}$$

The second term related to $E_2(q)$ present a gap at $q = 0$.
The integration is not straightforward and we need to perform a numerical calculation after substracting the proper counterterms, after a change of variables we recognize by series develop of the integrand the divergent terms e we compute the quantity: $I = \frac{1}{2}\int_0^\infty dq E_2(q)$

$$I = \frac{A^{\frac{5}{2}}}{2^{\frac{3}{2}}\pi^2}\int_0^\infty dx\sqrt{x}\left\{\sqrt{x(x+2)+\frac{B}{A^2}} - \underbrace{(x+1+\frac{\frac{B}{A^2}-1}{2x})}_{counterterms}\right\}. \tag{2.37}$$

where A and B are defined in (2.30) and (2.31).

It easy to prove that $\frac{B}{A^2} < 1$ and since the result must be real for stability, $\frac{B}{A^2} > 0$ and this result gives a lower limit for the chemical potential:

$$\mu > 2\omega_R\eta \tag{2.38}$$

2.2.3 Small Rabi approximation

We now consider the case of a little Rabi coupling constant [45]. The procedure is to take until first order the Taylor expansion of the (2.37) centered in $\omega_R = 0$.
Doing that we have

$$\begin{aligned} I = \frac{\sqrt{\eta^5\mu^5}}{\sqrt{8}\pi^2}\int_0^\infty dx\sqrt{x}\sqrt{x(x+2)}+ \\ +\frac{\sqrt{\eta^5\mu^5}}{\sqrt{32}\eta\mu\pi^2}\omega_R\int_0^\infty dx\frac{4+10(\eta+2)x+5(\eta+2)x^2}{\sqrt{x+2}} \end{aligned} \tag{2.39}$$

so, rearranging the formula

$$I = \frac{8}{15\pi^2}(\eta\mu)^{\frac{5}{2}} + \frac{\sqrt{\eta^5\mu^5}}{\sqrt{2}\eta\mu\pi^2}\omega_R\underbrace{\int_0^\infty \frac{dx}{\sqrt{x+2}}}_{A}+$$

$$+\frac{5\sqrt{\eta^5\mu^5}}{2\eta\mu\pi^2}(\eta+2)\omega_R\underbrace{\int_0^\infty dx\frac{x}{\sqrt{x+2}}}_{B} + \frac{5\sqrt{\eta^5\mu^5}}{4\eta\mu\pi^2}(\eta+2)\omega_R\underbrace{\int_0^\infty dx\frac{x^2}{\sqrt{x+2}}}_{C}$$

and finally, after regularizing (A), (B), (C) using dimensionless units we finally obtain the energy density of the system:

$$\frac{\mathcal{E}}{E_B/a^3} = \pi(1+\eta)\bar{n}^2 - \bar{\omega}_R\bar{n} + \frac{8}{15\pi^2}[2\pi\bar{n}(1+\eta)]^{\frac{5}{2}} + \frac{8}{15\pi^2}[2\pi\bar{n}(1-\eta)]^{\frac{5}{2}} + \frac{14}{3\pi^2}\bar{\omega}_R[2\pi\bar{n}(1+\eta)]^{\frac{3}{2}} \tag{2.40}$$

where $\bar{n} = na^3$, $E_B = 1/a^2$, $\bar{\mu} = \mu a^2$ and $\bar{\omega_R} = \omega_R a^2$.
This approximation is in perfect agreement with the numerical results for small ω_R. We obtained the so-called Lee-Huang-Yang terms for the equation of state. Notice that the Larsen equation of state appears with $\omega_R = 0$ [46].

This formula is not just a further grade of approximation for the mean field result, in fact the presence of the fluctuations gives stability of our system in regions of the phase diagram forbidden in the M-F configuration. We have seen before that $\varepsilon > -1$.

For $\varepsilon < -1$ we can notice that the term proportional to $[2\pi\bar{n}(1+\eta)]^{\frac{5}{2}}$ becomes immaginary. This fact cause dissipation, and no instabilities affect the quantum system. In this region it can be neglected, and minimizing the equation (2.40) we find a local minimum of the theory.

$$\bar{n}_- = \frac{5\sqrt{\pi}|1+\eta|}{32\sqrt{2}(1+|\eta|)^{\frac{5}{2}}}(1 - \frac{1792\bar{\omega_R}}{15\pi^2}\frac{(1+|\eta|)^4}{(1+\eta)^2})^2. \tag{2.41}$$

We notice that the last formula provides an upper limit for the Rabi frequency, for larger ω_R we have instability.

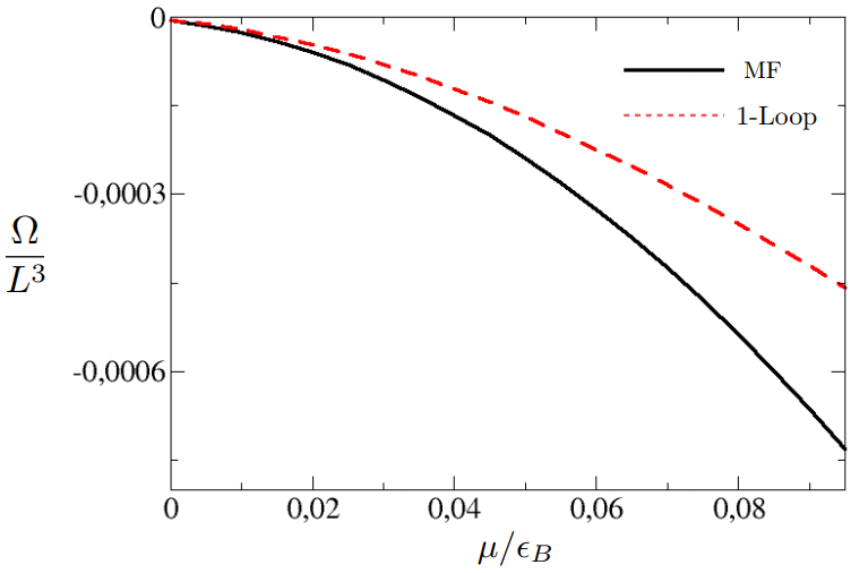

Figure 2.3: Grand potential as a function of the chemical potential. Black solid line represents the mean-field approximation. In the red-dashed line the beyond-mean-field corrections are included.

2.3 Droplet phase

In this section we characterize the droplet phase. As seen in the previous section the existence of quantum fluctuations can prevent the collapse of the Bose mixture. The idea is to define a complex field $\phi(\vec{x},t)$, such that $n(\vec{x},t) = |\phi(\vec{x},t)|^2$, for a finite number of particles N. It must satisfy the normalization condition $N = \int d^3x\ n(\vec{x},t)$. The dynamics of $\phi(\vec{x},t)$ is driven by the following real-time effective action:

$$S_{eff} = \int dt\ d^3x\ [i\bar{\phi}^*\partial_t\bar{\phi} - \frac{|\nabla\bar{\phi}|^2}{2} - \mathcal{E}_{eff}(|\bar{\phi}|^2)]. \tag{2.42}$$

where

$$\mathcal{E}_{eff}(|\bar{\phi}|^2) = -\bar{n}^2\pi|1+\eta||\bar{\phi}|^4 + \frac{256\sqrt{\pi}}{15}\bar{n}^{5/2}|\bar{\phi}|^5 + \frac{112\omega_R}{3\sqrt{\pi}}\bar{n}^{3/2}|\bar{\phi}|^3. \tag{2.43}$$

As done for equation (2.40) we rescaled all the quantities in order to have dimensionless parameters. In detail, $\bar{n} = na^3$, $|\phi| = \sqrt{n}|\bar{\phi}|$, $\bar{\mu} = \mu a^2$ and $\bar{\omega}_R = \omega_R a^2$. We can proceed with a variational approach, making a gaussian ansatz:

$$\bar{\phi}(\vec{r}) = \frac{\sqrt{\bar{N}}}{(\pi\bar{\sigma}^2)^{3/4}}e^{-r^2/2\bar{\sigma}^2}. \tag{2.44}$$

Inserting equation (2.44) in (2.43), the energy density becomes function of the droplet size σ. After minimazing the energy varying the size parameter, we can plot the density profile of the droplet.

Starting from the effective action in equation (2.43), it is possible to search for a stationary solution solving numerically the Gross-Pitaevskii equation (GPE) varying the number of particles. Such solution corresponds to a self-bound spherical droplet whose radial width increases by increasing the number of atoms.

$$i\frac{\partial\bar{\phi}}{\partial t} = [-\frac{\nabla^2}{2} - \bar{\mu} - \bar{\omega_R} - 2\pi\bar{n}^2|1+\eta||\bar{\phi}|^2 + \frac{128\sqrt{\pi}}{3}\bar{n}^{3/2}|\bar{\phi}|^5 + \frac{56\bar{\omega_R}}{\sqrt{\pi}}\sqrt{\bar{n}}|\bar{\phi}|]\ \bar{\phi}. \tag{2.45}$$

In the last expression we used rescaled time and space coordinates: $t \to ta^2$ and $\vec{r} \to \vec{r}/a$.

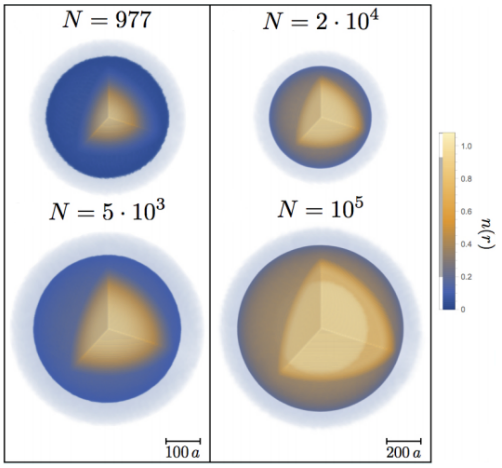

Figure 2.4: Three dimensional density profile of the droplet.

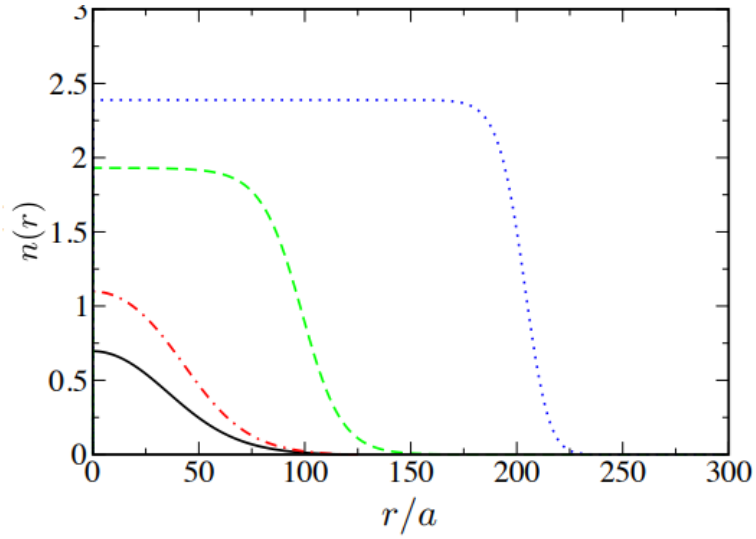

Figure 2.5: Density profile of the droplet. Here we consider $\omega_R = 2\pi \cdot$ 1kHz and $\eta = 0.5$. Black solid: metastable (positive energy) droplet for N = 546. Red dot-dashed: N = 10^3, Green dashed: N = 10^4, Blue dashed- double dotted: N = 10^5

As we can see in fig. 2.5, for a very large number of atoms the plateau of the density profile approaches the thermodynamic density given by equation (2.41). For low number of particles a solution doesn't exist.

To go further in the study of the dynamics of the droplet we adopt a new parametrization for the ϕ field:

$$\bar{\phi}(\vec{r},t) = \frac{\sqrt{\bar{N}}}{(\pi\bar{\sigma}_1^2\bar{\sigma}_2^2\bar{\sigma}_3^2)^{3/4}} \prod_{i=1}^{3} \exp[-r^2/2\bar{\sigma}_i + i\bar{\beta}_i r^2]. \tag{2.46}$$

Doing so we obtain an energy functional which depends on the four parameters $\vec{\bar{\sigma}}=\vec{\bar{\sigma}}(t)$ and $\bar{\beta}=\bar{\beta}(t)$.

$$\bar{U}(\vec{\bar{\sigma}}) = \frac{E}{N} = \frac{1}{2}\sum_{i=1}^{3}\frac{1}{2\sigma_i^2} - \frac{|1+\eta|N}{2\sqrt{2\pi}(\bar{\sigma}_1\bar{\sigma}_2\bar{\sigma}_3)} + \alpha\frac{(1+|\eta|)^{5/2}N^{3/2}}{(\bar{\sigma}_1\bar{\sigma}_2\bar{\sigma}_3)^{3/2}} + \gamma\frac{(1+|\eta|)^{3/2}\bar{\omega_R}N^{1/2}}{(\bar{\sigma}_1\bar{\sigma}_2\bar{\sigma}_3)^{1/2}} \tag{2.47}$$

where $\alpha = \frac{128}{75\sqrt{5}\pi^{7/4}}$ and $\gamma = \frac{112}{9\sqrt{3}\pi^{5/4}}$.

In the static case, the critical point of the potential energy is for $\bar{\sigma}_1 = \bar{\sigma}_2 = \bar{\sigma}_3$ so even in absence of external trap the ground state of the system has spherical symmetry solution. For small number of particles we find a metastable region where $\bar{U}(\vec{\bar{\sigma}})$ has a local minimum with positive energy, the global minimum corresponding to zero energy for a dispersed gas with zero density.
Interestingly, tuning the Rabi coupling to large there is a density region for which we can move from the stable phase into the unstable phase, as shown with the red-dashed line for N = 1200 particles in Fig.2.6.
Rabi coupling works so as an additional tool to tune the stability properties of the droplet.

In order to take into account the dynamics of excitations of the droplet above the ground state we need to calculate the Euler-Lagrangian equations of the theory asso-

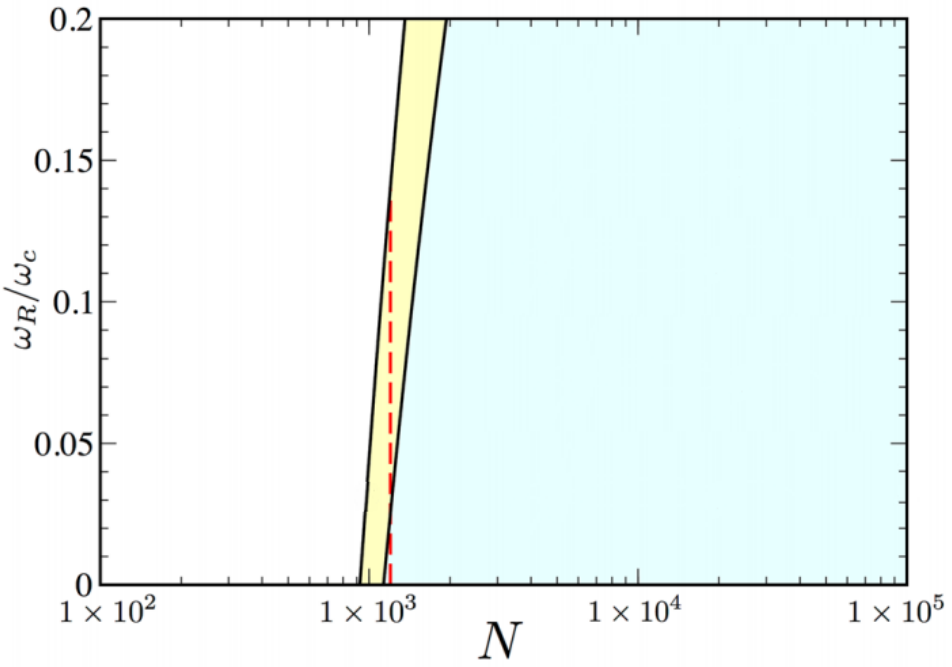

Figure 2.6: Stability diagram of the droplet phase. We observe three phases: a stable droplet-phase region (light green) of spherical self-bound droplets, a metastable droplet phase (yellow) and an unstable phase (white).

ciated with the effective potential in (2.47), [47].

$$\begin{cases} \bar{\beta}_i = \frac{\dot{\bar{\sigma}}_i}{2\bar{\sigma}_i} \\ \\ \ddot{\bar{\sigma}}_i = -\frac{\partial \bar{U}(\bar{\sigma}_1,\bar{\sigma}_2,\bar{\sigma}_3)}{\partial \bar{\sigma}_i}. \end{cases} \tag{2.48}$$

It is important to emphasise that once we solve the second equation in (2.48), we get automatically the time evolution of the $\bar{\beta}_i$ parameters.

The low-energy collective excitations of the self-bound droplet are investigated by solving the eigenvalues problem for the Hessian matrix of the potential energy given by (2.47).

$$\bar{U}_{ij}(\vec{\bar{\sigma}}) = \frac{\partial^2}{\partial\bar{\sigma}_i\partial\bar{\sigma}_j}\bar{U}(\vec{\bar{\sigma}}) = \begin{pmatrix} U_{11} & U_{12} & U_{13} \\ U_{21} & U_{22} & U_{23} \\ U_{31} & U_{32} & U_{33}. \end{pmatrix} \tag{2.49}$$

After taking the derivatives one finds the following matrix elements.
The diagonal terms are

$$\bar{U}(\vec{\bar{\sigma}})_{ii} = \frac{3}{2\bar{\sigma}_i^4} - \frac{|1+\eta|N}{\sqrt{2\pi}(\bar{\sigma}_1\bar{\sigma}_2\bar{\sigma}_3)\bar{\sigma}_i\bar{\sigma}_j} + \frac{9\alpha}{4}\frac{(1+|\eta|)^{5/2}N^{3/2}}{(\bar{\sigma}_1\bar{\sigma}_2\bar{\sigma}_3)^{3/2}\bar{\sigma}_i\bar{\sigma}_j} + \frac{1\gamma}{4}\frac{(1+|\eta|)^{3/2}\bar{\omega_R}N^{1/2}}{(\bar{\sigma}_1\bar{\sigma}_2\bar{\sigma}_3)^{1/2}\bar{\sigma}_i\bar{\sigma}_j} \tag{2.50}$$

while the off-diagonal terms read

$$\bar{U}(\vec{\bar{\sigma}})_{i\neq j} = -\frac{|1+\eta|N}{2\sqrt{2\pi}(\bar{\sigma}_1\bar{\sigma}_2\bar{\sigma}_3)\bar{\sigma}_i^2} + \frac{15\alpha}{4}\frac{(1+|\eta|)^{5/2}N^{3/2}}{(\bar{\sigma}_1\bar{\sigma}_2\bar{\sigma}_3)^{3/2}\bar{\sigma}_i^2} + \frac{3\gamma}{4}\frac{(1+|\eta|)^{3/2}\bar{\omega_R}N^{1/2}}{(\bar{\sigma}_1\bar{\sigma}_2\bar{\sigma}_3)^{1/2}\bar{\sigma}_i^2}. \tag{2.51}$$

After this, it is easy to solve the eigenvalue problem. The lowest excitation frequencies are so

$$\omega_1^2 = \bar{U}_{11} + 2\bar{U}_{12} \tag{2.52}$$

$$\omega_2^2 = \bar{U}_{11} - \bar{U}_{12}. \tag{2.53}$$

The eigenvector of frequency ω_1 is $v_M = (1,1,1)$: this excitation corresponds to a monopole oscillation, the breathing mode, which represents an expansion of the droplet over the three spatial dimensions.
To the frequency ω_2 corresponds two linearly independent eigenvectors $v_Q = (v_x, v_y, 1)$,

with $sgn(v_x) = -sgn(v_y)$. This excitation corresponds instead to a quadrupole oscillation.

In fig.(2.7) we plot the collective oscillation frequencies as a function of the number of particles, both for the monopole frequency and the quadrupole oscillation. As we expect, below $N \approx 977$ the droplet doesn't exist.

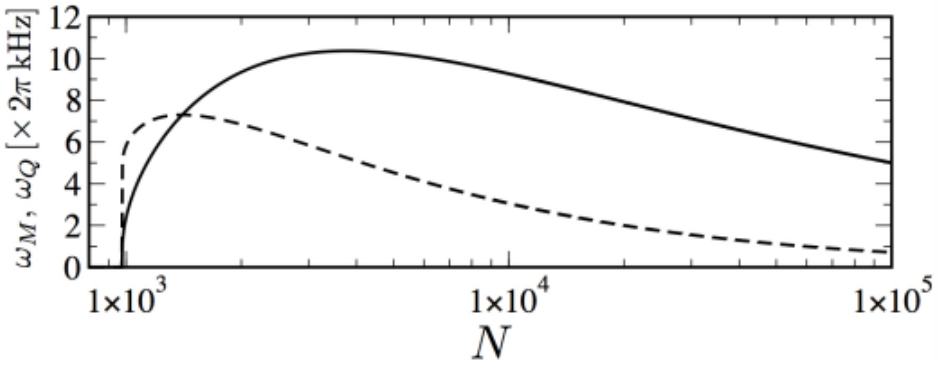

Figure 2.7: Frequency of collective modes as a function of the number of particles. Solid line represents monopole oscillation. Dashed line represents quadrupole oscillation

In fig.(2.8) we plot instead the collective oscillation frequencies as a function of the Rabi coupling, both for $N = 2 \cdot 10^3$ and $N = 10^5$. For these two plots we considered $|1 + \eta| = 0.5$ which corresponds to a critical Rabi frequency $\omega_c/2\pi = 31.8$ kHz.

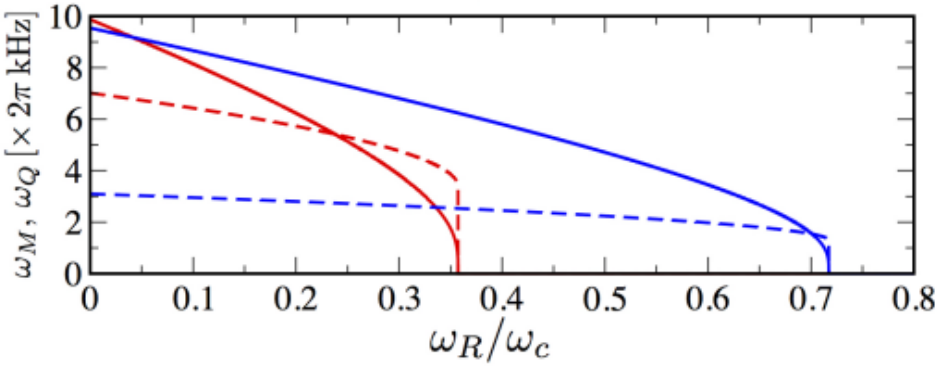

Figure 2.8: Frequency of collective modes as a function of the number of particles. Solid line represents monopole oscillation. Dashed line represents quadrupole oscillation. Red line is for $N = 2 \cdot 10^3$ and blue line for $N = 10^5$ (blue).

2.4 Experimental observation

A future candidate for the detection of the droplet in the presence of Rabi interaction is a gas of ^{39}K. After populating the hyperfine states $|F = 1, m_F = 0\rangle$ and $|F = 1, m_F = -1\rangle$, using a Feshbach resonance of $B \approx 54.5\ G$ it is possible to tune the two intra-component scattering lengths at the same value of $\approx 40\ a_0$. The corresponding inter-component scattering length is $\approx -60\ a_0$ [48, 49]. For a Rabi coupling of $\omega_c/2\pi = 1$ kHz and a number of particles of $N = 10^5$ we expect a droplet of FWHM $\approx 1.45\ \mu m$.

Chapter 3

Two component Rabi-coupled Fermi gas

In this section we investigate the properties of a system of Rabi-coupled ultracold fermionic atoms. As done in the previous chapter, we adopt functional integration methods: starting from the standard action of BCS theory we add a Rabi coupling term between the two fermionic fields and we work with a perturbative point of view, starting from the simple mean-field approximation and going beyond including quantum fluctuations. After calculating the single particle energy spectrum we get the grand potential in the mean field approximation: taking derivatives of it the gap equation and the number equation are obtained. The gap equation present a non-trivial dependence to Rabi frequency and this fact leads to a considerably change of the low temperature properties of the gas. The discussion of these new features are done in the BCS-BEC crossover framework. At the end of the chapter we provide the analytical corrections which must be included to the grand-potential to evaluate correctly the crossover, especially for the deep BEC regime of the quantum gas.

3.1 Functional integration and Hubbard-Stratonovich transformation

According with the functional integration formalism, the grand canonical partition function Z of interacting Rabi-coupled fermions at temperature T, contained in a volume L^3 can be written as:

$$Z = \int D[\Psi\bar{\Psi}] e^{-\int_0^\beta d\tau \int d^3x \; S[\Psi\bar{\Psi}]} \tag{3.1}$$

where the action reads

$$S[\Psi\bar{\Psi}] = \int_0^\beta d\tau \int d^3x \sum_{\sigma=\uparrow,\downarrow} \bar{\Psi}_\sigma(\partial_\tau - \frac{\nabla^2}{2m} - \mu)\Psi_\sigma + \omega_R(\bar{\Psi}_\uparrow\Psi_\downarrow + \bar{\Psi}_\downarrow\Psi_\uparrow) - g\bar{\Psi}_\downarrow\Psi_\uparrow\bar{\Psi}_\uparrow\Psi_\downarrow. \tag{3.2}$$

$\Psi_\sigma(\vec{x},\tau)$ and $\bar{\Psi}_\sigma(\vec{x},\tau)$ are anti-commuting Grassman field variables.
They replace, in the path integral approach, the fermionic field operators [32-33].
The fields $\Psi_\sigma(\vec{x},\tau)$ and $\bar{\Psi}_\sigma(\vec{x},\tau)$ satisfy antiperiodic boundary conditions in the imaginary time [49]:

$$\begin{aligned} \Psi_\sigma(\vec{x},\tau) &= -\Psi_\sigma(\vec{x},\tau+\beta) \\ \bar{\Psi}_\sigma(\vec{x},\tau) &= -\bar{\Psi}_\sigma(\vec{x},\tau+\beta) \end{aligned} \tag{3.3}$$

We are interested in the grand potential, given by the following formula:

$$\Omega = -\frac{1}{\beta}\log(Z). \tag{3.4}$$

This quantity contains all the thermodynamic information of our quantum gas, so the calculation of the partition function is the main issue.

An important idea is to introduce an auxiliary complex field $\Delta(\vec{x},\tau)$, the so-called pairing field.
The partition function can be rewritten adding a functional integration over the complex field and doing so an effective but still exact action appears, equivalent to

(2).

$$Z = \int D[\Psi\bar{\Psi}\ \Delta\bar{\Delta}] \exp[-\int_0^\beta d\tau \int d^3x \frac{|\Delta(x)|^2}{g} - \frac{1}{2}\bar{\Psi}(x)G^{-1}\Psi(x)\ ] \tag{3.5}$$

where

$$\Psi = \begin{bmatrix} \Psi_\uparrow \\ \bar{\Psi}_\downarrow \\ \Psi_\downarrow \\ \bar{\Psi}_\uparrow \end{bmatrix}$$

is the extended Nambu-Gor'kov spinor.

$$G^{-1} = \begin{bmatrix} -\partial_\tau + \frac{\nabla^2}{2m} + \mu & \Delta & -\omega_R & 0 \\ \bar{\Delta} & -\partial_\tau - \frac{\nabla^2}{2m} - \mu & 0 & \omega_R \\ -\omega_R & 0 & \partial_\tau + \frac{\nabla^2}{2m} + \mu & -\Delta \\ 0 & \omega_R & -\bar{\Delta} & -\partial_\tau - \frac{\nabla^2}{2m} - \mu \end{bmatrix} \tag{3.6}$$

The interaction beetween fermions is mediated by Δ, the price to pay for having quadratic terms in the fermionic fields is the inclusion of the auxiliary pairing [33]. The simplest approximation is to impose on the bosonic field to be a costant (standard mean-field approach).
Doing this we can get the mean field BCS equations, as shown in the following chapter.

3.2 Mean field approximation

The simplest approximation scheme consists in completely ignoring the fluctuations, imposing the pairing field to be constant $\Delta(\vec{x}, \tau) = \Delta_0$. With this choice, the action is greatly simplified: the field Δ loses the dynamics and it is replaced by its saddle-point value Δ_0.

It is well known that the function $G(k, i\omega)$ (the Fourier transform of the inverse of the operator in equation (3.6)) is a meromorphic function of $i\omega$ with simple poles at the exact excitation energies of the interacting and Rabi-coupled system, corresponding to a momentum $\vec{k}$ [49].
After a Wick rotation, in order to have real frequencies, the energy spectrum is so

$$\omega_{\pm}(\vec{k}) = \sqrt{\varepsilon(\vec{k})^2 + \Delta_0^2} \pm \omega_R \tag{3.7}$$

where $\varepsilon(\vec{k}) = \frac{\vec{k}^2}{2m} - \mu$.

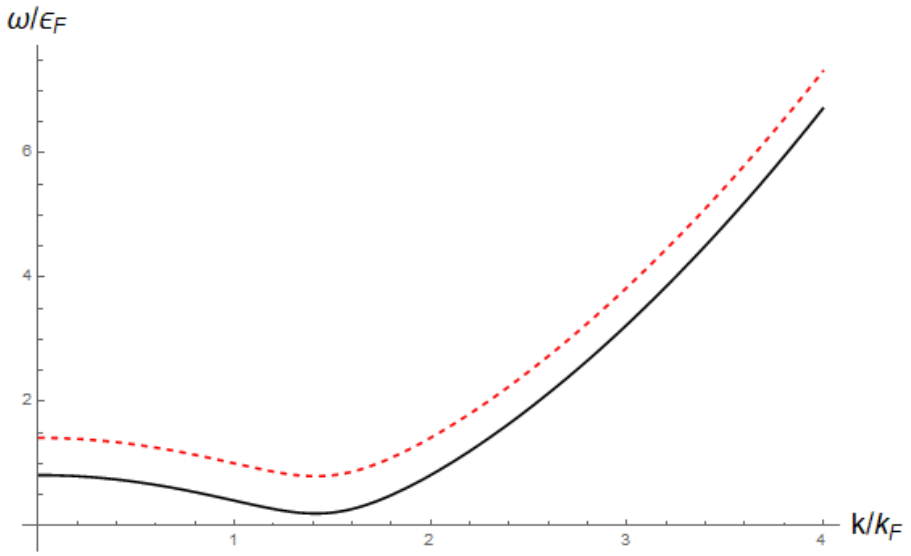

Figure 3.1: Bogoliubov quasi-particles excitations. ω_- is represented by black solid line, ω_+ by red-dashed line. Here we use $\Delta_0/\varepsilon_F = 0.5$, $\omega_R/\varepsilon_F = 0.3$.

The gap equation is then found evaluating the trace over both Nambu space and momentum space

$$\frac{1}{g}\bar{\Delta} = \frac{1}{2}Tr(G \begin{bmatrix} 0 & 1 & 0 & 0 \\ 0 & 0 & 0 & 0 \\ 0 & 0 & 0 & -1 \\ 0 & 0 & 0 & 0 \end{bmatrix}) = \frac{1}{2}tr(G_{2,1} - G_{4,3}) \tag{3.8}$$

where

$$G_{12}(k) = -G_{34} = -\Delta_0 \frac{(i\omega_n)^2 - \varepsilon(\vec{k})^2 - \Delta_0^2 + \omega_R^2}{((i\omega)^2 - \omega_-^2)((i\omega)^2 - \omega_+^2)}. \tag{3.9}$$

Using (3.8) and (3.9) we get

$$\frac{1}{g} = -\frac{1}{\beta\Omega}\sum_{\vec{k},i\omega} \frac{(i\omega)^2 - E(\vec{k})^2 + \omega_R^2}{((i\omega)^2 - \omega_-^2)((i\omega)^2 - \omega_+^2)} \tag{3.10}$$

with $E(\vec{k}) = \sqrt{\varepsilon(\vec{k})^2 + \Delta_0^2}$.

Adding and substracting $\omega\hbar\omega_R$ we obtain:

$$\frac{1}{g} = -\frac{1}{2\beta\Omega}\sum_{\vec{k},i\omega}(\frac{1}{(i\omega - \omega_R)^2 - E(\vec{k})^2} + \frac{1}{(i\omega + \omega_R)^2 - E(\vec{k})^2}). \tag{3.11}$$

Summing over the Matsubara frequencies we finally obtain the *gap equation*

$$\frac{1}{g} = \frac{1}{4\Omega}\sum_{\vec{k}} \frac{tanh[\frac{\beta}{2}(E(\vec{k}) + \omega_R)]}{E(\vec{k})} + \frac{tanh[\frac{\beta}{2}(E(\vec{k}) - \omega_R)]}{E(\vec{k})}. \tag{3.12}$$

As expected, the standard BCS results are reproduced setting $\omega_R = 0$.

At this point, in order to get the grand potential in the mean field approximation, from (3.5) we evaluate the trace both in the momentum and Nambu space.
After performing the summation over the fermionic Matsubara frequencies and after

taking $\Omega = -\frac{1}{\beta}\log(Z)$ we obtain the grand-potential

$$\Omega = V\frac{\Delta_0^2}{g} - \frac{1}{2\beta}\sum_{\vec{k}}\sum_{i=1}^{4}\log(1+e^{-\beta\omega_i(\vec{k})}) \tag{3.13}$$

where $\omega_1(\vec{k}) = \sqrt{\varepsilon(\vec{k})^2+\Delta_0^2} - \omega_R$, $\omega_2(\vec{k}) = \sqrt{\varepsilon(\vec{k})^2+\Delta_0^2} - \omega_R$, $\omega_3(\vec{k}) = -\omega_1(\vec{k})$ and $\omega_4(\vec{k}) = -\omega_2(\vec{k})$.

Once we have the grand potential it is possible to derive all the thermodynamical properties of the system, including the gap equation (3.13), which is obtained minimizing

$$\frac{\partial\Omega}{\partial\Delta_0} = 0. \tag{3.14}$$

3.3 BCS theory with Rabi

3.3.1 Critical temperature

Following the BCS theory common procedure, in order to calculate T_c we set the order parameter to 0. The density of state is imposed to be constant in a thin shell of energy (in the standard BCS theory, with electrons in a solid, it is of the order of the Debye frequency) around the Fermi energy level.
Therefore, we can integrate the (3.12) after a change of variable

$$\frac{1}{g} = \frac{\rho_F}{2}\int_0^{\omega_C}\frac{d\varepsilon}{\varepsilon}[tanh(\frac{\varepsilon-\omega_R}{2T_c}) + tanh(\frac{\varepsilon+\omega_R}{2T_c})] \tag{3.15}$$

where ω_C is the cutoff frequency and $\rho_F = \frac{k_F}{\pi^2}$ is the density of state at the Fermi surface.
It is necessary to introduce a cutoff: equation (3.14) present a divergence if we perform integration over all the momenta.

After the derivation of critical temperature we show the usual method to avoid this problem in the context of ultracold atoms.
According with the theory of scattering, redefining the scattering length we can introduce a counter-term that regularizes the integral [35]. So, at the end of the chapter we enlight the map between the cutoff frequency and physical parameters such as Fermi energy.

Naming $\tilde{\omega}_C = \frac{\omega_C}{2T_c}$ and $\tilde{\omega}_R = \frac{\omega_R}{2T_c}$, after appropriate changes of variables

$$\frac{1}{g\rho_F} = \frac{1}{2}\int_0^{\tilde{\omega}_C-\tilde{\omega}_R} dx \frac{tanh(x-\tilde{\omega}_R)}{x+\tilde{\omega}_R} + \frac{1}{2}\int_0^{\tilde{\omega}_C+\tilde{\omega}_R} dx \frac{tanh(x+\tilde{\omega}_R)}{x-\tilde{\omega}_R}.$$

In the limit $\frac{\omega_C-\omega_R}{2T_c} >> 1$

$$\begin{aligned}\frac{1}{g\rho_F} \approx & \frac{1}{2}[tanh(x)log(|x+\tilde{\omega}_R|)]_0^{\tilde{\omega}_C-\tilde{\omega}_R} + \frac{1}{2}[tanh(x)log(|x-\tilde{\omega}_R|)]_0^{\tilde{\omega}_C+\tilde{\omega}_R} \\ & - \int_0^{\infty} dx \frac{log(|x^2-\tilde{\omega_R}^2|)}{2cosh^2(x)}.\end{aligned}$$

The critical temperature of the BCS theory in the presence of Rabi interaction can be found inverting the following identity:

$$\frac{1}{g\rho_F} = log[\frac{\omega_C}{2T_c\mathcal{F}(\frac{\omega_R}{2T_c})}] \tag{3.16}$$

where we defined

$$\mathcal{F}(\frac{\omega_R}{2T_c}) := \exp(\int_0^{\infty} dx \frac{log(|x^2-\tilde{\omega}_R^2|)}{2cosh^2(x)}). \tag{3.17}$$

In the case of $\omega_R = 0$ it is straightforward to prove that $\mathcal{F}(0) = \frac{\pi}{4e^{\gamma_E}}$, where $\gamma_E \approx 0.577$ is the well known Euler constant.
In this case we have the standard Rabi-less critical temperature:

$$T_c = \frac{2e^{\gamma_E}\omega_C}{\pi} e^{-\frac{1}{g\rho_F}}. \tag{3.18}$$

In ultracold quantum gas systems we can obtain BCS superconductivity tuning the

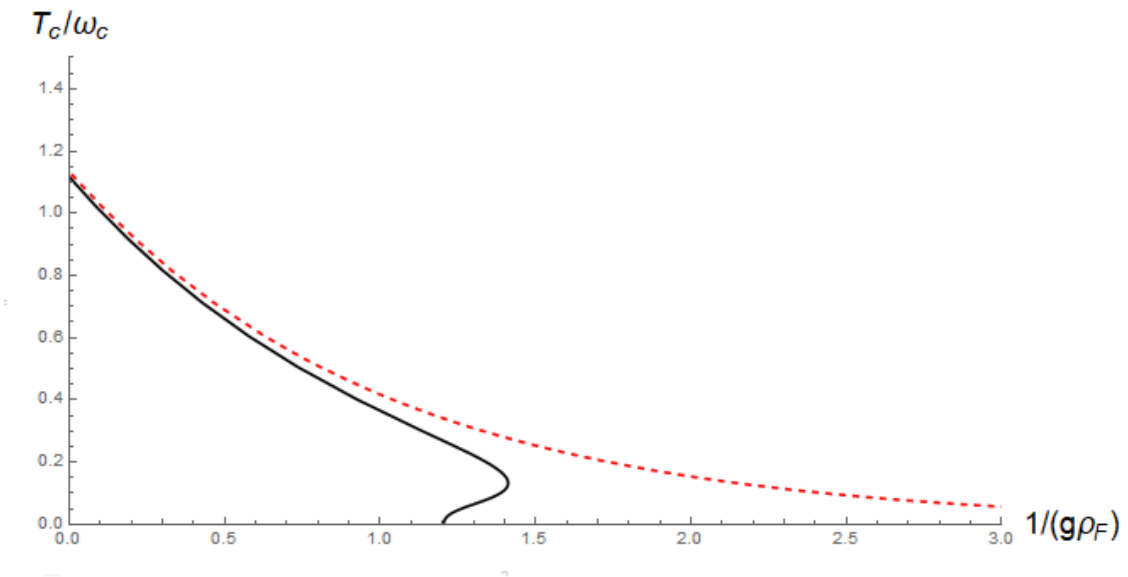

Figure 3.2: Critical temperature as a function of the strength of the interaction. Red-dashed line: $\omega_R = 0$ case. Black solid line: $\omega_R/\omega_C = 0.3$. Turning on the Rabi coupling we can notice that below a certain value of the coupling g the presence of Rabi inhibits the superconductivity.

scattering length to small negative values using Feshbach resonance. In such case we don't have a cutoff energy like the Debye frequency in classical supercondictivity theory on solids.

As mentioned above, according to the theory of the scattering, we can renormalize the costant g in this way:

$$\frac{1}{g} = \frac{1}{g_r} + \int \frac{d^3k}{(2\pi)^3}\frac{1}{k^2}. \tag{3.19}$$

In order to get the mapping between the cutoff frequency and Fermi energy we consider equation (3.13), after setting $\omega_R = 0$ and using the renormalization of the constant we solve the Rabi-less gap equation

$$\frac{1}{g_r} = \int \frac{d^3k}{(2\pi)^3}[\frac{tanh[\frac{\beta}{2}(\varepsilon(\vec{k}) - \mu)]}{2(\varepsilon(\vec{k}) - \mu)} - \frac{1}{2\varepsilon(\vec{k})}]. \tag{3.20}$$

For a weakly-interacting Fermi gas near-zero temperature, the chemical potential is well approximated by the Fermi energy $\mu = \varepsilon_F$.

Naming $x = \frac{\varepsilon}{\mu}$ and $y = \frac{\beta\mu}{2}$ we get

$$\frac{1}{g_r} = \frac{k_F}{2\pi^2}\int_0^\infty dx\sqrt{x}[\frac{tanh[y(x-1)]}{2(x-1)} - \frac{1}{2x}]. \tag{3.21}$$

In order to perform analytical calculations we split the formula using

$$\frac{\sqrt{x}}{x-1} = \frac{1}{\sqrt{x}+1} + \frac{1}{x-1}$$

After rearranging the equation (3.20) and using $\beta\mu >> 1$ we get

$$\frac{1}{g_r} = \frac{k_F}{2\pi^2}(-2 + log(4) + \gamma_E + log(\frac{2\beta_c\varepsilon_F}{\pi})). \tag{3.22}$$

The critical temperature is then

$$T_c = \frac{8e^{\gamma_E - 2}\varepsilon_F}{\pi}e^{-\frac{1}{g\rho_F}}. \tag{3.23}$$

Comparing equation (3.22) with equation (3.17) we can make a map between the cutoff frequency and the Fermi energy

$$\omega_C = 4e^{-2}\varepsilon_F. \tag{3.24}$$

We see that the low temperature assumption is justified in the case of weakly interactions $g \to 0$, because then the critical temperature becomes exponentially small. In the weakly-interacting limit we can also ignore self-energy effects, such that the zero-temperature ideal gas result $\mu = \varepsilon_F$ is justified to a very good approximation [36].

Temporarily, we don't discuss the physical meaning of the last results. In section 3.4 we deeply investigate the interpretation of gap equation of Rabi-coupled systems with

a more rigorous analysis, discussing the BCS-BEC crossover of ultracold atoms.

3.3.2 Number equation

The gap equation in (3.12) encodes all the information of the superconductivity in the approximation of a static and homogeneous system. To solve it anyway we must specify the chemical potential: it can be fixed inverting the so-called *number equation*.

We start from the grand potential obtained in section 3.2,

$$\Omega = V\frac{\Delta_0^2}{g} - \frac{1}{2\beta}\sum_{\vec{k}}\sum_{i=1}^{4}\log(1+e^{-\beta\omega_i(\vec{k})})$$

Using the well known thermodynamic relation for the number of particles

$$N = -\frac{\partial\Omega}{\partial\mu} = -\sum_{\vec{k}}[-1+\frac{1}{2}\sum_{i=1}^{4}\frac{\partial\omega_i}{\partial\mu}\frac{e^{-\beta\omega_i}}{1+e^{-\beta\omega_i}}]$$

and since $\omega_3 = -\omega_1$ e $\omega_4 = -\omega_2$

$$= \sum_{\vec{k}}[1+\frac{1}{2}\sum_{i=\pm}^{2}\frac{\partial\omega_i}{\partial\mu}(\frac{e^{+\beta\omega_i}}{1+e^{\beta\omega_i}} - \frac{e^{-\beta\omega_i}}{1+e^{-\beta\omega_i}})]$$

$$= \sum_{\vec{k}} 1+\frac{1}{2}\sum_{i=\pm}^{2}\frac{\partial\omega_i}{\partial\mu}tanh(\frac{\beta}{2}\omega_i)$$

$$\frac{\partial\omega_\pm}{\partial\mu} = -\frac{\varepsilon(\vec{k})}{E(\vec{k})}.$$

Finally we obtain the number equation

$$N = \sum_{\vec{k}} 1 - \varepsilon(\vec{k}) \frac{tanh(\frac{\beta}{2}(E(\vec{k}) + \omega_R))}{2E(\vec{k})} - \varepsilon(\vec{k}) \frac{tanh(\frac{\beta}{2}(E(\vec{k}) - \omega_R))}{2E(\vec{k})} \tag{3.25}$$

3.3.3 Number equation at low critical temperature

We start from the number equation in (3.24) and we fix $\Delta_0 = 0$:

$$N = \sum_{\vec{k}} 1 - \frac{1}{2} tanh(\frac{\beta}{2}(\frac{\vec{k}^2}{2} - \mu + \omega_R)) - \frac{1}{2} tanh(\frac{\beta}{2}(\frac{\vec{k}^2}{2} - \mu - \omega_R)).$$

We define $\mu_+ = \mu + \omega_R$ e $\mu_- = \mu - \omega_R$, and after a change of variable we get

$$n = \frac{1}{\sqrt{2}\pi^2} \int d\varepsilon \sqrt{\varepsilon} [1 - \frac{1}{2} tanh(\frac{\beta}{2}(\varepsilon - \mu_-)) - \frac{1}{2} tanh(\frac{\beta}{2}(\varepsilon - \mu_-))].$$

At this point we notice that in the Rabi-less case the chemical potential must be positive, while for $\omega_R > 0$ this is not true.
Therefore we compute the contributions separately.

For $\mu > \omega_R$ taking the limit $\beta >> 1$

$$n = \frac{1}{\sqrt{2}\pi^2} (2 \int d\varepsilon \sqrt{\varepsilon} \Theta(\mu_- - \varepsilon) + \int d\varepsilon \sqrt{\varepsilon} \Theta(\varepsilon - \mu_-) \Theta(\mu_+ - \varepsilon))$$

so

$$n = \frac{\sqrt{2}}{3\pi^2} [(\mu - \omega_R)^{3/2} + (\mu + \omega_R)^{3/2}] \tag{3.26}$$

For $-\omega_R < \mu < \omega_R$, taking the limit

$$n = \frac{1}{\sqrt{2}\pi^2} \int d\varepsilon \sqrt{\varepsilon} \Theta(\mu_+ - \varepsilon)$$

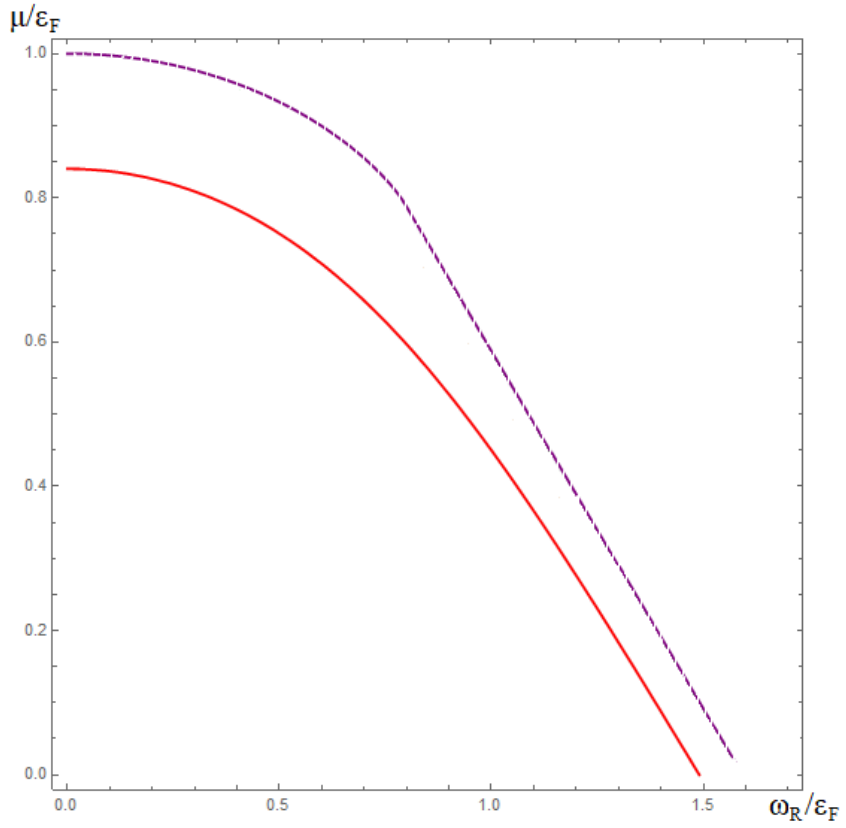

Figure 3.3: Numerical solution of the number equation in (3.24) at fixed density of particle $3\pi^2 n/2^{3/2} = 1$. Red solid line: non-zero temperature case with $T/T_F = 0.4$. Purple-dashed line $T/T_F = 0$ case.

$$n = \frac{\sqrt{2}}{3\pi^2}(\mu + \omega_R)^{3/2} \tag{3.27}$$

The case $\mu < -\omega_R$ gives no contributions to the number equation.

Mixing it all together

$$n = \frac{\sqrt{2}}{3\pi^2}[(\mu - \omega_R)^{3/2}\Theta(\mu - \omega_R) + (\mu + \omega_R)^{3/2}]. \tag{3.28}$$

When we set $\omega_R = 0$ we recover the well-known relation $\mu = \frac{1}{2}(3\pi n)^{2/3}$ [49].

3.4 BCS-BEC crossover

BCS theory involves the condensation of Cooper pairs, which are extended bosonic objects with typical dimensions being determined by the coherence length ε_0.
Tuning the strength of the effective interaction beetween electrons, making it stronger, the Cooper pairs shrink and they end up forming tightly bound bosonic molecules.

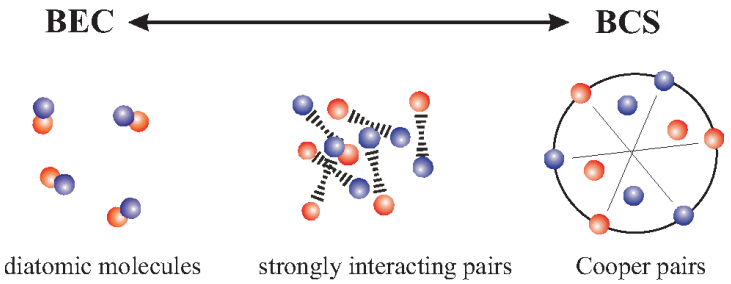

Figure 3.4: BCS-BEC crossover. With Feschbach resonance technique it is possible to tune the interaction between fermions. Starting from the weakly bound BCS Cooper pairs we reach the strongly bound BEC regime, passing through the unitary limit.

The crossover can be obtained changing the s-wave scattering length beetween atoms using the Fano-Feschbach technique: as explained in Section 1.2.1, changing the intensity of an external magnetic field it is possible to show that the strength of the coupling beetween atoms changes. The scattering length can be choose very large or very small and it can also change sign.

In 2004 the BCS-BEC crossover has been observed in ultracold quantum gases made of two fermionic component ^{40}K or ^{6}Li alkali atoms. It has been proved that Feshbach molecules created by fermions are much more stable than the bosons, with time scales consistent with the Bose-Einstein condensation [52], [53].

The aim of this section is to report the main results of the BCS-BEC crossover theory using the path integral formalism. Firstly we present the classical theory of the crossover, then we provide the extension of the theory in the presence of a Rabi coupling. We start from a mean-field approximation (with the aid of the

results already obtained in section 3.2) and then we go beyond it including bosonic excitations in our calculations, both for the standard crossover and for Rabi-coupled extension. We report the numerical solutions obtained for the mean-field gap equation and we provide the physical interpretation of the results. At the end of the section we present the calculations necessary to include the quantum fluctuations, underling the physical differences between the two degrees of approximation.

3.4.1 Mean field theory of the standard BCS-BEC crossover

Starting from the action

$$S[\Psi\bar{\Psi}] = \int_0^\beta d\tau \int d^3x \sum_{\sigma=\uparrow,\downarrow} \bar{\Psi}_\sigma(\partial_\tau - \frac{\nabla^2}{2m} - \mu)\Psi_\sigma - g\bar{\Psi}_\downarrow\Psi_\uparrow\bar{\Psi}_\uparrow\Psi_\downarrow \tag{3.29}$$

using an Hubbard-Stratonovich transformation in the Cooper-pairs channel and after summing over the fermionic field we get:

$$S_\Delta = \int_0^\beta d\tau \int d^3x \frac{|\Delta(x)|^2}{g} - Tr[\log(G^{-1})]. \tag{3.30}$$

Firstly, setting the pairing $\Delta = \Delta_0$ it is straightforward to evaluate the trace in the momentum space. After summing over the Matsubara frequencies $\omega_n = \frac{(2n+1)\pi}{\beta}$ we can obtain the mean-field grand potential:

$$\Omega_0 = -\frac{1}{\beta}\log(Z_0) = -\frac{\Delta_0^2}{g}L^3 + \sum_{\vec{k}}(\frac{\vec{k}^2}{2m} - \mu - E_{sp}(\vec{k}) - \frac{2}{\beta}log(1 + e^{\beta E_{sp}(\vec{k})}) \tag{3.31}$$

where the single particle spectrum given by

$$E_{sp}(\vec{k}) = \sqrt{(\frac{\vec{k}^2}{2m} - \mu)^2 + \Delta_0^2} \tag{3.32}$$

represent the poles of the propagator in the costant energy gap approximation.
From the grand potential it is easy to get the gap equation. Imposing the stationarity

condition $\frac{\partial\Omega(\Delta_0)}{\partial\Delta_0} = 0$ we get the well-known relation

$$\frac{1}{g} = \frac{1}{2\Omega}\sum_{\vec{k}} \frac{tanh[\frac{\beta}{2}(E(\vec{k})]}{E(\vec{k})} \tag{3.33}$$

where $E(\vec{k}) = \sqrt{\varepsilon(\vec{k})^2 + \Delta_0^2}$

The summation must be taken over all the momenta, from 0 to ∞. The gap equation in (3.32) diverges, so the coupling g must be renormalized according with the theory of scattering, as already explain in section 3.18.

$$\frac{1}{g} = -\frac{1}{4\pi a_F} + \int \frac{d^3k}{(2\pi)^3}\frac{1}{k^2}$$

where a_F is the scattering lenght for fermions.

The second equation we need to solve is called number equation. It is the thermodynamic relation between the number of particles and the chemical potential.

$$n(\mu) = -\frac{\partial\Omega(\mu)}{\partial\mu}. \tag{3.34}$$

The procedure to obtain the critical temperature of the system as a function of our basic parameter, the scattering length, is the following: firstly, at fixed temperature, we invert the number equation, with the intention to express the chemical potential as a function of density of particle and the temperature $\mu(n, T)$. After this, the gap equation can be plotted, in order to highlight the relation between scattering length and temperature at fixed number of particles.

3.4.2 Beyond mean field contributions for standard BCS-BEC crossover

At this point we consider the pair field as the sum of a mean-field constant term and a time and space dependent fluctuations field:

$$\begin{aligned} \Delta(\vec{x},\tau) &= \Delta_0 + \eta(\vec{x},\tau) \\ \Delta^*(\vec{x},\tau) &= \Delta_0 + \eta^*(\vec{x},\tau) \end{aligned} \tag{3.35}$$

where $\eta(x,\tau)$ is the abovementioned complex field which describes pairing fluctuations.
The action in (3.30) can be rewrititten as:

$$S_\Delta = \int_0^\beta d\tau \int d^3x \ \frac{|\Delta_0 + \eta(\vec{x},\tau)|^2}{g} - Tr[log(G_0^{-1} + K)] \tag{3.36}$$

where, in the momentum space:

$$G_0^{-1}(k) = \begin{bmatrix} i\omega_n - \varepsilon(\vec{k}) & \Delta_0 \\ \Delta_0 & i\omega_n + \varepsilon(\vec{k}) \end{bmatrix} \tag{3.37}$$

and

$$K(k, k+q) = \begin{bmatrix} 0 & \eta(q) \\ \eta^*(-q) & 0 \end{bmatrix}. \tag{3.38}$$

The idea is to rewrite the trace in order to have a perturbative expansion in the fluctuations field:

$$Tr[\log(G_0^{-1} + K)] = Tr[\log(G_0^{-1})] - Tr[G_0 K] + \frac{1}{2} Tr[(G_0 K)^2] - ...$$

At second order we can include the quantum fluctuations in the action $S_\Delta = S_0 + S_g$.

The partition function in this case is the product of a mean-field term and a fluctuations term $Z = Z_0 Z_g$, so the grand potential is

$$\Omega = \Omega_0 + \Omega_g. \tag{3.39}$$

Considering only quadratic terms in $\eta(\vec{x}, \tau)$

$$S_\Delta = \int_0^\beta d\tau \int d^3x \frac{|\Delta_0|^2}{g} - Tr[log(G_0^{-1})] + \frac{|\eta(x)|^2}{g} + \frac{1}{2} Tr[(G_0 K)^2]. \tag{3.40}$$

Inverting G_0^{-1} we get

$$\begin{aligned} G_{11}(k) &= -G_{22}(-k) = \frac{i\omega_n + \varepsilon(\vec{k})}{(i\omega_n)^2 - \varepsilon(\vec{k})^2 - \Delta_0^2} \\ G_{12}(k) &= G_{21}(k) = -\frac{\Delta_0}{(i\omega_n)^2 - \varepsilon(\vec{k})^2 - \Delta_0^2}. \end{aligned} \tag{3.41}$$

The term $+\frac{\Delta_0}{g}(\eta(x) + \eta^*(x)) - Tr[G_0 K]$ vanishes using saddle point condition.
In fact

$$Tr[G_0 K] = tr[G_{12}(\eta^* + \eta)] = \frac{1}{\beta L^3} \sum_Q (\eta^*(Q) + \eta(-Q)) \sum_k G_{12}(k) \tag{3.42}$$

where $k = (\omega_n, \vec{k})$ e $Q = (\Omega_n, \vec{q})$ are four-vectors, the first one related to fermionic frequencies, the second to bosonic ones.
So, we focus on the gaussian fluctuations:

$$S_g = \int_0^\beta d\tau \int d^3x + \frac{|\eta(\vec{x}, \tau)|^2}{g} + \frac{1}{2} Tr[(G_0 K)^2] \tag{3.43}$$

Evaluating the trace in the momentum space

$$\frac{1}{2} Tr[(G_0 K)^2] = \frac{1}{2} tr[G_{12}\eta^* G_{12}\eta^* + G_{12}\eta G_{12}\eta + 2G_{11}\eta G_{22}\eta^*]. \tag{3.44}$$

The first term is:

$$\frac{1}{2}tr[G_{12}\eta^* G_{12}\eta^*] = \frac{1}{2\beta L^3}\sum_Q \eta^*(Q)\sum_k G_{12}(k)G_{12}(k+Q)\eta^*(-Q) \tag{3.45}$$

the second

$$\frac{1}{2}tr[G_{12}\eta G_{12}\eta] = \frac{1}{2\beta L^3}\sum_Q \eta(Q)\sum_k G_{12}(k)G_{12}(k+Q)\eta(-Q) \tag{3.46}$$

and finally the third one reads

$$tr[G_{12}\eta G_{12}\eta] = \frac{1}{\beta L^3}\sum_Q \eta^*(Q)\sum_k G_{11}(k+Q)G_{22}(k)\eta(Q). \tag{3.47}$$

The physics of the fluctuations is so encoded in the quadratic form represented by the matrix $\mathbb{M}$, which is the inverse propagator of Gaussian fluctuations of pairs.

$$S_g = \frac{1}{2}\sum_Q (\eta^*(Q)\eta(-Q))\mathbb{M}(\mathbb{Q})\begin{pmatrix}\eta(Q)\\ \eta^*(-Q)\end{pmatrix} \tag{3.48}$$

Using (3.41) for the calculation of the trace (3.44) we obtain:

$$\mathbb{M}_{11}(Q) = \frac{1}{g} + \frac{1}{\beta L^3}\sum_{i\omega_n,\vec{k}} \frac{i\omega_n + i\Omega_n + \varepsilon(\vec{k}+\vec{q})}{(i\omega_n + i\Omega_n)^2 - \varepsilon(\vec{k}+\vec{q})^2 - \Delta_0^2}\frac{i\omega_n - \varepsilon(\vec{k})}{(i\omega_n)^2 - \varepsilon(\vec{k})^2 - \Delta_0^2} \tag{3.49}$$

$$\mathbb{M}_{12}(Q) = \frac{1}{\beta L^3}\sum_{i\omega_n,\vec{k}} \frac{\Delta_0^2}{[(i\omega_n + i\Omega_n)^2 - \varepsilon(\vec{k}+\vec{q})^2 - \Delta_0^2][(i\omega_n)^2 - \varepsilon(\vec{k})^2 - \Delta_0^2]} \tag{3.50}$$

and it is easy to prove that $\mathbb{M}_{11}(Q) = \mathbb{M}_{22}(-Q)$ e $\mathbb{M}_{12}(Q) = \mathbb{M}_{21}(Q)$.
As we can see, the matrix is a complicated object, it is related to bosonic excitations but inside it there are fermionc exicitations.

Solving

$$det[log(\mathbb{M}(\mathbb{Q}))] = 0 \tag{3.51}$$

it is possibile to find E_{coll}, which represent the spectrum of bosonic collective excita-

tions, as solution of the equation above.

In the deep Bose-Einstein condensate regime you can find that the gaussian fluctuations grand potential can be written in this way

$$\Omega_g \simeq \frac{1}{2}\sum_{\vec{q}} E_{coll}(\vec{q}) + \frac{1}{\beta}\sum_{\vec{q}} log(1 - e^{\beta E_{coll}(\vec{q})}). \tag{3.52}$$

Formally we are able to write the grand potential, which depends on temperature T, volume L^3, chemical potential μ and energy gap parameter Δ_0. The latter can be fixed imposing the stationarity of the mean field grand-potential (saddle point)

$$\frac{\partial \Omega_0}{\partial \Delta_0} = 0. \tag{3.53}$$

The number equation gets a new contribution:

$$n = -\frac{\partial \Omega}{\partial \mu} = -\frac{\partial \Omega_0}{\partial \mu} - \frac{\partial \Omega_g}{\partial \mu} - \frac{\partial \Omega_g}{\partial \Delta_0}\frac{\partial \Delta_0}{\partial \mu}. \tag{3.54}$$

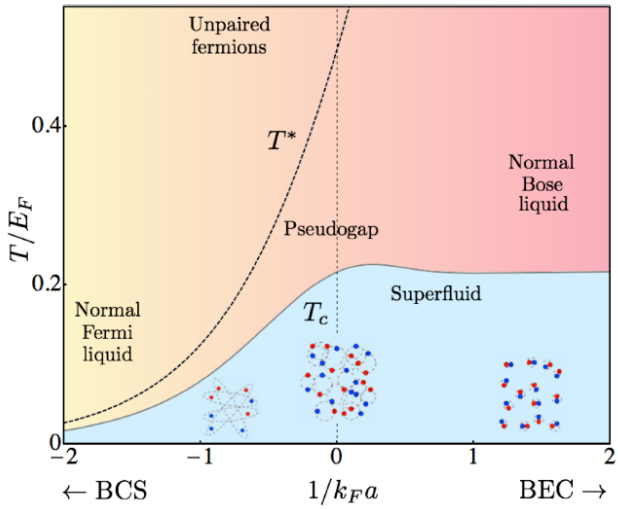

Figure 3.5: Differences between mean-field and beyond-mean-field approximation for the BCS-BEC crossover

3.4.3 Mean field theory of BCS-BEC crossover with Rabi interaction

In section 3.2 we have obtained the mean-field grand potential setting the pairing field constant and performing the summation over the Matsubara frequencies.

$$\Omega = V\frac{\Delta_0^2}{4\pi a_F} - \frac{1}{2\beta}\sum_{\vec{k}}\sum_{i=1}^{4}\log(1+e^{-\beta\omega_i(\vec{k})})$$

where $\omega_1(\vec{k}) = \sqrt{\varepsilon(\vec{k})^2+\Delta_0^2} - \omega_R$, $\omega_2(\vec{k}) = \sqrt{\varepsilon(\vec{k})^2+\Delta_0^2} - \omega_R$, $\omega_3(\vec{k}) = -\omega_1(\vec{k})$ and $\omega_4(\vec{k}) = -\omega_2(\vec{k})$.

The main ingredient for the crossover is the regularization of the grand potential: the basic idea is to take summation over all the momenta; redefining the coupling between particles we obtain a finite quantity which represent the grand potential for ultracold atoms.
Moreover, doing this the scattering length between fermions can also be positive, so we are able to investigate the so-called BEC regime.

$$-\frac{1}{4\pi a_F} = \frac{1}{g_r} + \int\frac{d^3k}{(2\pi)^3}\frac{1}{k^2}$$

where a_F is the scattering length for fermions.

Minimizing the grand potential we get the gap equation

$$-\frac{1}{4\pi a_F} = \int\frac{d^3k}{(2\pi)^3}[\frac{tanh[\frac{\beta}{2}(E(\vec{k})-\omega_R)]}{2E(\vec{k}}) + \frac{tanh[\frac{\beta}{2}(E(\vec{k})+\omega_R)]}{2E(\vec{k})} - \frac{1}{2\varepsilon(\vec{k})}] \quad (3.55)$$

where $E(\vec{k}) = \sqrt{\varepsilon(\vec{k})^2+\Delta_0^2}$.

In order to find the critical temperature of the system we fix the gap to 0, so we can plot the temperature as a function of the controlled parameter a_F, solving numerically (3.56) and number equation in (3.25) we obtain

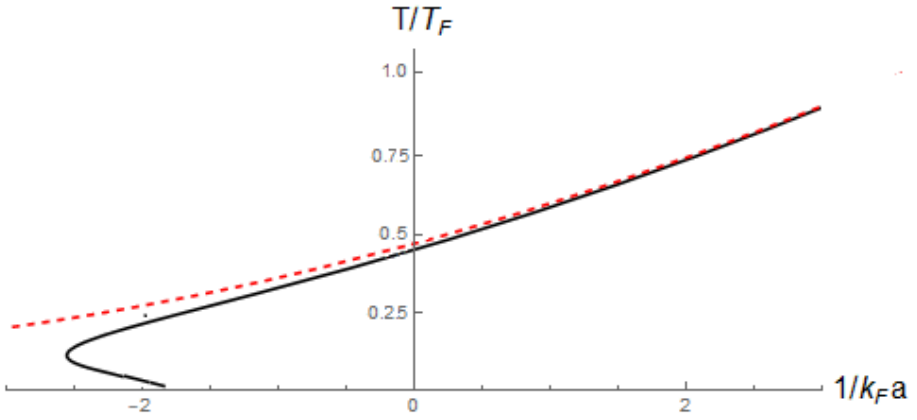

Figure 3.6: Critical temperature of the BCS-BEC crossover in mean field approximation. Solid black line: ω_R/ε_F=0.6. Red-dashed line: ω_R/ε_F=0

The presence of Rabi affects the BCS regime. As we can see in equation (3.56) or more generally in equation (3.13), for large temperature the Rabi frequency becomes irrelevant, so, at mean field level, in the BEC regime the presence of Rabi is not interesting.
In figure 3.6 we can notice how for a specific scattering length we have an inversion of the curve: for a specific region there seems to be two critical temperatures.
Later in this chapter we will show that one of the two solution (the lower one) does not represent a minimum of the theory.
The result is that the Rabi interaction does not allow superconductivity if the strength of the interaction is under a certain threshold.

At this point using gap equation (3.56) at very low temperature together with number equation we can plot the energy gap as a function of scattering length (Fig. 3.7).

As noticed before during the analysis of the critical temperature, for the Rabi-coupled case there is a particular range of scattering lengths which allows two solutions for the gap. As stressed before and as we show later on, the lower solution is a maximum for the grand potential. So, there is a threshold of energy gap below which there is no superconductivity. This threshold in the low temperature limit coincides exactly with the energy ω_R. The Rabi breaks the Cooper pairs which have an energy lower than that provided by the Rabi coupling.

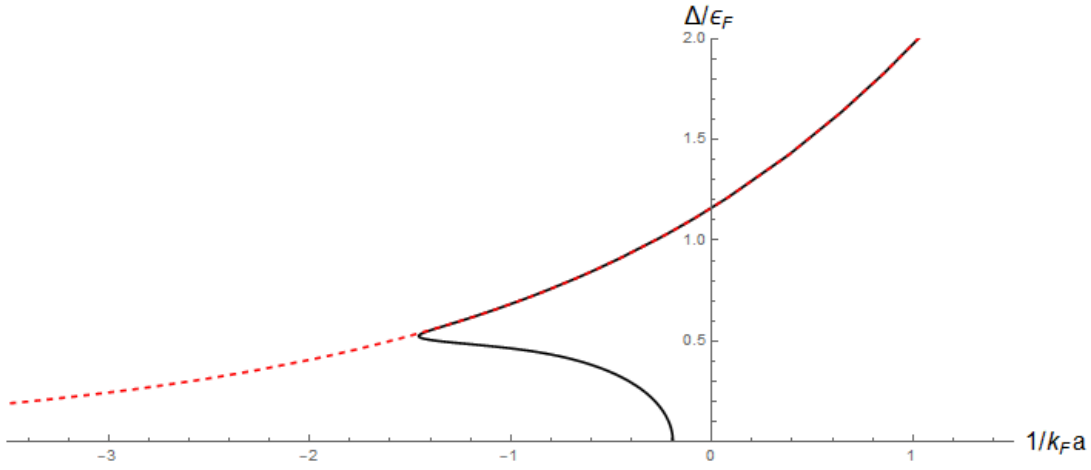

Figure 3.7: Energy gap as a function of scattering lenght. Solid black line: ω_R/ε_F=0.5. Red-dashed line: ω_R/ε_F=0

Let us start with the grand potential in equation (3.13), our intention is to take the $T = 0$ limit. So,

$$\begin{aligned}\Omega =& V\frac{\Delta_0^2}{4\pi a_F} - \frac{1}{2\beta}\sum_{\vec{k}}\log(1+e^{-\beta(E(\vec{k})+\omega_R)}) - \frac{1}{2\beta}\sum_{\vec{k}}\log(1+e^{-\beta(E(\vec{k})-\omega_R)}) \\ &- \frac{1}{2\beta}\sum_{\vec{k}}\log(1+e^{+\beta(E(\vec{k})+\omega_R)}) - \frac{1}{2\beta}\sum_{\vec{k}}\log(1+e^{+\beta(E(\vec{k})+\omega_R)}).\end{aligned} \tag{3.56}$$

With Rabi, the low temperature limit is not trivial, in fact we need to specify in which conditions we have $E(\vec{k}) - \omega_R > 0$ (the quantity $E(\vec{k}) + \omega_R$ is always positive):

$$\begin{cases} if & \Delta_0 > \omega_R & \forall\vec{k} \\ if & \Delta_0 < \omega_R & |\vec{k}| < k_-, |\vec{k}| > k_+ \end{cases}$$

where

$$\begin{aligned} k_- &= \sqrt{2(\mu - \sqrt{\omega_R^2 - \Delta_0^2})} \\ k_+ &= \sqrt{2(\mu + \sqrt{\omega_R^2 - \Delta_0^2})}. \end{aligned} \tag{3.57}$$

Finally, taking the limit $\beta \to +\infty$ in equation (3.56) we get the grand potential at

zero temperature,

if $\Delta_0 > \omega_R$

$$\Omega = V\frac{\Delta_0^2}{4\pi a_F} - \sum_{\vec{k}} E(\vec{k}) \tag{3.58}$$

if $\Delta_0 < \omega_R$

$$\Omega = V\frac{\Delta_0^2}{4\pi a_F} - \sum_{|\vec{k}|<k_-,|\vec{k}|>k_+} E(\vec{k}) - \sum_{k_-<|\vec{k}|<k_+} \omega_R \tag{3.59}$$

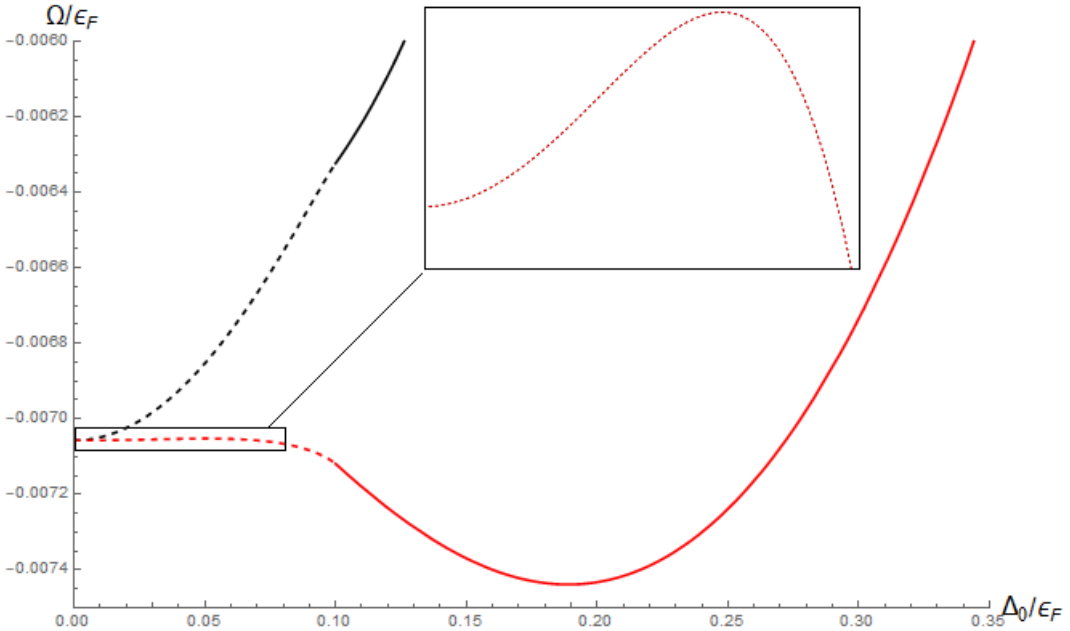

Figure 3.8: Grand potential at zero temperature as a function of the gap parameter. ω_R/ε_F=0.9. Black line: $1/(k_F a_F)$ = -1.5, red line: $1/(k_F a_F)$ = -0.5. The dashed line represents the case $\Delta_0 < \omega_R$.

As we pointed out before, the Rabi affects considerably the zero point energy of the fermions in BCS regime. It splits the grand potential into two separate contributions.

3.4.4 Beyond mean field BEC-BCS crossover with Rabi interaction

Starting from the action

$$S[\Psi\bar{\Psi}] = \int_0^\beta d\tau \int d^3x \sum_\sigma \bar{\Psi}_\sigma(\partial_\tau - \frac{\nabla^2}{2m} - \mu)\Psi_\sigma + \hbar\omega_R(\bar{\Psi}_\uparrow\Psi_\downarrow + \bar{\Psi}_\downarrow\Psi_\uparrow) - g\bar{\Psi}_\downarrow\Psi_\uparrow\bar{\Psi}_\uparrow\Psi_\downarrow \tag{3.60}$$

we next use a Hubbard-Stratanovich transformation with an auxiliary field $\Delta(\vec{x},\tau)$ which couples to $\bar{\Psi}_\uparrow\bar{\Psi}_\downarrow$ and after summing over the fermionic field we get:

$$S_\Delta = \int_0^\beta d\tau \int d^3x \frac{|\Delta(x)|^2}{g} - Tr[log(\frac{1}{2}G^{-1})]. \tag{3.61}$$

As done for the Rabi-less cas we rewrite the order parameter as a sum of a mean-field term and a fluctuations term $G^{-1} = G_0^{-1} + K$, where

$$K(k,k+q) = \begin{bmatrix} 0 & \eta(q) & 0 & 0 \\ \eta^*(-q) & 0 & 0 & 0 \\ 0 & 0 & 0 & -\eta(q) \\ 0 & 0 & -\eta^*(-q) & 0 \\ . & & & \end{bmatrix} \tag{3.62}$$

Inverting G_0^{-1} we get

$$G(k) = \begin{bmatrix} G_{11} & G_{12} & G_{13} & G_{14} \\ G_{21} & G_{22} & -G_{14} & G_{24} \\ G_{13} & -G_{14} & G_{11} & -G_{12} \\ G_{14} & G_{24} & -G_{12} & G_{22} \\ . & & & \end{bmatrix} \tag{3.63}$$

where

$$
\begin{aligned}
G_{11}(k) &= \frac{1}{\beta L^3}\frac{(i\omega_n+\varepsilon(\vec{k}))((i\omega_n)^2-\varepsilon(\vec{k})^2-\Delta_0^2)-\omega_R(i\omega_n-\varepsilon(\vec{k}))}{((i\omega)^2-\omega_-^2)((i\omega)^2-\omega_+^2)}\\
G_{12}(k) &= -\frac{1}{\beta L^3}\Delta_0\frac{(i\omega_n)^2-\varepsilon(\vec{k})^2-\Delta_0^2+\omega_R^2}{((i\omega)^2-\omega_-^2)((i\omega)^2-\omega_+^2)}\\
G_{22}(k) &= \frac{1}{\beta L^3}\frac{(i\omega_n-\varepsilon(\vec{k}))((i\omega_n)^2-\varepsilon(\vec{k})^2-\Delta_0^2)-\omega_R(i\omega_n+\varepsilon(\vec{k}))}{((i\omega)^2-\omega_-^2)((i\omega)^2-\omega_+^2)}\\
G_{13}(k) &= -\frac{1}{\beta L^3}\omega_R\frac{\omega_R^2-(i\omega_n+\varepsilon(\vec{k}))^2-\Delta_0^2}{((i\omega)^2-\omega_-^2)((i\omega)^2-\omega_+^2)}\\
G_{23}(k) &= \frac{1}{\beta L^3}\omega_R\frac{\omega_R^2-(i\omega_n-\varepsilon(\vec{k}))^2-\Delta_0^2}{((i\omega)^2-\omega_-^2)((i\omega)^2-\omega_+^2)}\\
G_{14}(k) &= \frac{1}{\beta L^3}\frac{i\omega_n\omega_R\Delta_0}{((i\omega)^2-\omega_-^2)((i\omega)^2-\omega_+^2)}
\end{aligned}
\tag{3.64}
$$

the functions ω_- e ω_+ are defined in (3.13) and they represent the excitation spectrum of the Rabi-coupled BCS system.
The key issue is to calculate the traces

$$
\begin{aligned}
\frac{1}{2}Tr[(GK)^2] =& tr(G_{12}\eta^*G_{12}\eta^*+G_{14}\eta^*G_{14}\eta^*+G_{12}\eta G_{12}\eta)\\
&+G_{14}\eta G_{14}\eta-2G_{13}\eta G_{24}\eta^*+2G_{11}\eta G_{22}\eta^*).
\end{aligned}
\tag{3.65}
$$

Let us consider the terms individually:

$$
\begin{aligned}
tr(G_{12}\eta^*G_{12}\eta^*+G_{14}\eta^*G_{14}\eta^*) =& \frac{1}{\beta L^3}\sum_Q\eta^*(Q)(\sum_k G_{12}(k)G_{12}(k+Q)\\
&+G_{14}(k)G_{14}(k+Q))\eta^*(-Q)
\end{aligned}
\tag{3.66}
$$

$$
\begin{aligned}
tr(G_{12}\eta G_{12}\eta+G_{14}\eta G_{14}\eta) =& \frac{1}{\beta L^3}\sum_Q\eta(Q)(\sum_k G_{12}(k)G_{12}(k+Q)\\
&+G_{14}(k)G_{14}(k+Q))\eta(-Q)
\end{aligned}
\tag{3.67}
$$

$$2tr(G_{11}\eta G_{22}\eta^* - G_{13}\eta G_{24}\eta^*) = \frac{2}{\beta L^3}\sum_Q \eta^*(Q)(\sum_k G_{11}(k+Q)G_{22}(k+Q) - G_{13}(k+Q)G_{14}(k))\eta(Q) \tag{3.68}$$

Our intention is to rewrite the gaussian contributions in terms of a quadratic form:

$$S_g = \frac{1}{2}\sum_Q (\eta^*(Q)\eta(-Q))\mathbb{M}^{\omega_{\mathbb{R}}}(\mathbb{Q})\begin{pmatrix}\eta(Q)\\ \eta^*(-Q)\end{pmatrix}. \tag{3.69}$$

Rewriting the inverse of the fluctuations propagator as $\mathbb{M}^{\omega_{\mathbb{R}}}(\mathbb{Q}) = \mathbb{M}^{\omega_{\mathbb{R}}=0}(\mathbb{Q}) + \Omega(\mathbb{Q})$

$$\Omega(\mathbb{Q})_{11} = -\frac{1}{\beta L^3}\sum_k \omega_R^2\Big(\frac{(i\omega_n + i\Omega_n + \varepsilon(\vec{k}+\vec{q}))((i\omega_n+i\Omega_n)^2 - \varepsilon(\vec{k}+\vec{q})^2 - \Delta_0^2)(i\omega_n + \varepsilon(\vec{k}))}{((i\omega_n+i\Omega_n)^2-\omega_-^2)((i\omega_n+i\Omega_n)^2-\omega_+^2)((i\omega_n)^2-\omega_-^2)((i\omega_n)^2-\omega_+^2)}$$
$$\frac{(i\omega_n + i\Omega_n - \varepsilon(\vec{k}+\vec{q}))(i\omega_n^2 - \varepsilon(\vec{k})^2 - \Delta_0^2)(i\omega_n - \varepsilon(\vec{k}))}{((i\omega_n+i\Omega_n)^2-\omega_-^2)((i\omega_n+i\Omega_n)^2-\omega_+^2)((i\omega_n)^2-\omega_-^2)((i\omega_n)^2-\omega_+^2)}\Big)$$

$$\Omega(\mathbb{Q})_{12} = +\frac{1}{\beta L^3}\sum_k \omega_R^2\Delta_0^2\Big(\frac{(i\omega_n)^2 + (i\omega_n+i\Omega_n)^2 - \varepsilon(\vec{k})^2 - \varepsilon(\vec{k}+\vec{q})^2 - 2\Delta_0}{((i\omega_n+i\Omega_n)^2-\omega_-^2)((i\omega_n+i\Omega_n)^2-\omega_+^2)((i\omega_n)^2-\omega_-^2)((i\omega_n)^2-\omega_+^2)}$$
$$+\frac{i\omega_n(i\omega_n+i\Omega_n)}{((i\omega_n+i\Omega_n)^2-\omega_-^2)((i\omega_n+i\Omega_n)^2-\omega_+^2)((i\omega_n)^2-\omega_-^2)((i\omega_n)^2-\omega_+^2)}$$

The other matrix elements are $\Omega(\mathbb{Q})_{22} = \Omega(-\mathbb{Q})_{11}$ e $\Omega(\mathbb{Q})_{21} = \Omega(\mathbb{Q})_{12}$.

We obtained the analytical expression for the matrix elements of quantum fluctuations propagator.

Summing numerically over the Matsubara frequencies and momenta it could be possible to evaluate the entire crossover in the presence of the Rabi coupling. These calculations however are particularly demanding and they fall outside the scope of the thesis.

While in the mean-field approximation we showed that the Rabi interaction does not affect the physics of the the deep BEC regime, it may not be true for the collective

excitations. According with the standard BCS-BEC crossover theory, we expect that for small and positive scattering length the critical temperature approaches that of non-interacting bosons, calculated for Rabi case in section 2.1.

$$\frac{n}{2} = (\frac{T_{c,\omega_R}}{2\pi})^{\frac{3}{2}}[\zeta(3/2) + f(e^{\frac{-2\omega_R}{T_{c,\omega_R}}})] \tag{3.70}$$

where the function $f(z)$ is defined as:

$$f(z) = \sum_{n=1}^{\infty} \frac{z^n}{n^{\frac{3}{2}}}$$

We note that in equation (3.65) we used $\frac{n}{2}$, which is the density of diatomic bosonic molecules.

Appendix

Condensed number

In chapter 3 we investigated a system of interacting fermions in the presence of Rabi coupling. A fundamental quantity which is important to calculate is the condensate fraction. In this appendix we provide the analytical calculations that must be performed to evaluate numerically the condensate fraction [51], a result which is, however, out of the scope of the thesis. We calculated the singlet contribution and the triplet contribution, the latter is a peculiarity of the Rabi-coupled case.

Singlet contribution

$$N_0 = \frac{1}{\beta}\sum_{\vec{k}} |\sum_{i\omega} \langle \Psi^{\uparrow}(\vec{k})\Psi^{\downarrow}(-\vec{k})\rangle\,|^2 = \frac{1}{\beta}\sum_{\vec{k}} |\sum_{\omega} -G_{2,1} + G_{4,3}|^2$$

$$= \frac{\Delta_0^2}{\beta}\sum_{\vec{k}} |\sum_{i\omega} \frac{2(i\omega)^2 + 2\omega_R^2 - 2E(\vec{k})^2}{(\omega^2-\omega_-^2)(\omega^2-\omega_+^2)}|^2$$

now, adding and substracting $2i\omega\omega_R$

$$= \frac{\Delta_0^2}{\beta}\sum_{\vec{k}} |\sum_{i\omega} \frac{(\omega+\omega_R)^2 - E(\vec{k})^2 + (\omega-\omega_R)^2 - E(\vec{k})^2}{((i\omega)^2-\omega_-^2)((i\omega)^2-\omega_+^2)}|^2$$

$$= \frac{\Delta_0^2}{\beta} \sum_{\vec{k}} | \sum_{i\omega} \frac{1}{(i\omega + \omega_R)^2 - E(\vec{k})^2} + \frac{1}{(i\omega - \omega_R)^2 - E(\vec{k})^2} |^2.$$

Summing over the Matsubara frequencies

$$N_0 = \frac{\Delta_0^2}{4} \sum_{\vec{k}} [\frac{tanh(\frac{\beta}{2}(E(\vec{k}) + \omega_R))}{2E(\vec{k})} + \frac{tanh(\frac{\beta}{2}(E(\vec{k}) - \omega_R))}{2E(\vec{k})}]^2. \tag{3.71}$$

Triplet contribution

$$N_1 = \frac{1}{\beta} \sum_{\vec{k}} | \sum_{i\omega} \langle \Psi^{\uparrow}(\vec{k}) \Psi^{\uparrow}(-\vec{k}) \rangle |^2 = \frac{1}{\beta} \sum_{\vec{k}} | \sum_{\omega} G_{4,1} |^2$$

$$= \frac{\Delta_0^2}{\beta} \sum_{\vec{k}} | \sum_{i\omega} \frac{2i\omega\omega_R}{((i\omega)^2 - \omega_-^2)((i\omega)^2 - \omega_+^2)} |^2.$$

It is easy to prove that the down-down contribution is identical to the one above.

Adding and substracting $(i\omega)^2 + \omega_R^2 - E(\vec{k})^2$

$$N_1 = \frac{\Delta_0^2}{4\beta} \sum_{\vec{k}} | \sum_{i\omega} \frac{(i\omega)^2 + \omega_R^2 - E(\vec{k})^2 + 2i\omega\omega_R - ((i\omega)^2 + \omega_R^2 - E(\vec{k})^2 - 2i\omega\omega_R)}{((i\omega)^2 - \omega_-^2)((i\omega)^2 - \omega_+^2)} |^2$$

$$N_1 = \frac{\Delta_0^2}{16} \sum_{\vec{k}} [\frac{tanh(\frac{\beta}{2}(E(\vec{k}) + \omega_R))}{2E(\vec{k})} - \frac{tanh(\frac{\beta}{2}(E(\vec{k}) - \omega_R))}{2E(\vec{k})}]^2. \tag{3.72}$$

As mentioned at the begin of the section, this last contribute vanishes if we set $\omega_R = 0$.

Bibliography

[1] A. Einstein, Sitzber. Kgl. Preuss. Akad. Wiss., 261 (1924).

[2] P. Kapitsa, Nature 141, 74 (1938).

[3] J.F. Allen, A.D. Misener, Nature 141, 75 (1938).

[4] H.K. Onnes, Comm. Phys. Lab. Univ. Leiden, Nos. 119, 120, 122 (1911).

[5] W. Meissner, R. Ochsenfeld, Naturwiss. 21, 787 (1933).

[6] J. Bardeen, L.N. Cooper, J.R. Schrieffer, Phys. Rev. 108, 1175 (1957).

[7] J.G. Bednorz, K.A. Muller, Z. Phys. B ¨ 64, 189 (1986).

[8] M.H. Anderson, J.R. Ensher, M.R. Matthews, C.E. Wieman, E.A. Cornell, Science 269, 198 (1995).

[9] C.C. Bradley, C.A. Sackett, J.J. Tollett, R.G. Hulet, Phys. Rev. Lett. 75, 1687 (1995).

[10] K.B. Davis, M.O. Mewes, M.R. Andrews, N.J. van Druten, D.S. Durfee, D.M. Kurn, W. Ketterle, Phys. Rev. Lett. 75, 3969 (1995).

[11] A. J. Moerdijk, B. J. Verhaar, and A. Axelsson, Resonances in ultracold collisions of 6Li, 7Li, and 23Na, Phys. Rev. A 51, 4852 (1995).

[12] S. Inouye, M. R. Andrews, J. Stenger, H.-J. Miesner, D. M. Stamper-Kurn, and W. Ketterle, Observation of Feshbach resonances in a Bose-Einstein condensate, Science 392, 151 (1998).

[13] J. L. Roberts, N. R. Claussen, S. L. Cornish, E. A. Donley, E. A. Cornell, and C. E. Wieman, Controlled collapse of a Bose-Einstein Condensate, Phys. Rev. Lett. 86, 4211 (2001).

[14] E. A. Donley, N. R. Claussen, S. T. Thompson, and C. E. Wieman, Atommolecule cohorence in a Bose-Einstein Condensate, Nature 417, 529 (2002).

[15] C. Chin, A. J. Kerman, V. Vuletic, and S. Chu, ´ Sensitive Detection of Cold Cesium Molecules Formed on Feshbach Resonances, Phys. Rev. Lett. 90, 033201 (2003).

[16] J. Herbig, T. Kraemer, M. Mark, T. Webwr, C. Chin, H. C. Nägerl, and R. Grimm, Preparation of a Pure Molecular Quantum Gas, Science 301, 1510 (2003).

[17] C. A. Regal, C. Ticknor, J. L. Bohn, and D. S. Jin, Creation of ultracold molecules from a Fermi gas of atoms, Nature 424, 47 (2003).

[18] K. E. Strecker, G. B. Partridge, and R. G. Hulet, Conversion of an Atomic Fermi Gas to a Long-Lived Molecular Bose Gas, Phys. Rev. Lett. 91, 080406 (2003).

[19] J. Cubizolles, T. Bourdel, S. J. J. M. F. Kokkelmans, G. V. Shlyapnikov, and C. Salomon Production of Long-Lived Ultracold Li2 Molecules from a Fermi Gas, Phys. Rev. Lett. 91, 240401 (2003).

[20] S. Jochim, M. Bartenstein, A. Altmeyer, G. Hendl, C. Chin, J. Hecker Denschlag, and R. Grimm, Pure Gas of Optically Trapped Molecules Created from Fermionic Atoms, Phys. Rev. Lett. 91, 240402 (2003).

[21] B.D. Josephson, Phys. Lett. 1, 251 (1962) .

[22] A. Barone, G. Patern´o, Physics and Applications of the Josephson Effect (Wiley, New York, 1982) .

[23] G. Milburn, J. Corney, E. Wright, and D. Walls, Phys. Rev. A 55, 4318 (1997) .

[24] Inguscio, M.; Fallani, L. Atomic Physics: Precise Measurements and Ultracold Matter; Oxford University Press: Oxford, UK, 2013.

[25] Steck, D.A. Quantum and Atom Optics. Available online: http://steck.us/teaching (accessed on 11 April 2018).

[26] Smerzi, A., Trombettoni, A., Lopez-Arias, T. et al. Eur. Phys. J. B (2003).

[27] C. A. Regal, M. Greiner, and D. S. Jin. Observation of Resonance Condensation of Fermionic Atom Pairs. Phys. Rev. Lett., 92, 2004.

[28] M. W. Zwierlein, C. A. Stan, C. H. Schunck, S. M. F. Raupach, A. J. Kerman, and W. Ketterle. Condensation of Pairs of Fermionic Atoms near a Feshbach Resonance Phys. Rev. Lett., 92, 2004.

[29] A. J. Leggett, in Modern Trends in the Theory of Condensed Matter, edited by A. Pekalski and R. Przystawa Springer-Verlag, Berlin, 1980.

[30] D. M. Eagles, Phys. Rev. 186, 456 (1969).

[31] Abad M., Recati, A. A study of coherently coupled two-component Bose-Einstein condensates. Eur. Phys. J. D 67, 40053 (2013).

[32] N. Nagaosa, Quantum Field Theory in Condensed Matter Physics (Springer, 1999).

[33] A. Altland and B. Simons, Condensed Matter Field Theory (Cambridge Univ. Press, 2006).

[34] Armaitis, J., Stoof, H. T. C. Duine, R. A. Hydrodynamic modes of partially condensed Bose mixtures. Phys. Rev. A 91, 043641 (2015).

[35] Schakel, A. Boulevard of Broken Symmetries: Efective Field Teories of Condensed Matter. (World Scientifc, Singapore, 2008).

[36] Stoof, H. T. C., Dickerscheid, D. B. M. Gubbels, K. Ultracold Quantum Fields. (Springer, Dordrecht, 2009).

[37] Andersen, J. O. Teory of the weakly interacting Bose gas. Rev. Mod. Phys. 76, 599–639 (2004).

[38] Lellouch, S., Dao, T.-L., Kofel, T. Sanchez-Palencia, L. Two-component Bose gases with one-body and two-body couplings. Phys. Rev. A 88, 063646 (2013).

[39] Search, C. P., Rojo, A. G. Berman, P. R. Ground state and quasiparticle spectrum of a two-component Bose-Einstein condensate. Phys. Rev. A 64, 013615 (2001).

[40] Tommasini, P., de Passos, E. J. V., de Toledo Piza, A. F. R., Hussein, M. S.

Timmermans, E. Bogoliubov theory for mutually coherent condensates. Phys. Rev. A 67, 023606 (2003).

[41] Salasnich L., Toigo F. Zero-point energy of ultracold atoms. Phys. Rep. 640, 1–20 (2016).

[42] Petrov, D. S. Quantum Mechanical Stabilization of a Collapsing Bose-Bose Mixture. Phys. Rev. Lett. 115, 155302 (2015).

[43] Petrov, D. S. Ultradilute Low-Dimensional Liquids. Phys. Rev. Lett. 117, 100401 (2016).

[44] Diener, R. B., Sensarma, R. Randeria, M. Quantum fuctuations in the superfuid state of the BCS-BEC crossover. Phys. Rev. A 77, 023626 (2008).

[45] Butera, S., Öhberg, P. Carusotto, I. Black-hole lasing in coherently coupled two-component atomic condensates. arXiv:1702.07533v1 (2017).

[46] Larsen, D. M. Binary mixtures of dilute Bose gases with repulsive interactions at low temperatures. Ann. Phys. 24, 89–101 (1963).

[47] Pèrez-Garcia, V. M., Michinel, H., Cirac, J. I., Lewenstein, M. Zoller, P. Low Energy Excitations of a Bose-Einstein Condensate: ATime-Dependent Variational Analysis. Phys. Rev. Lett. 77, 5320 (1996).

[48] D'Errico, C. et al. Feshbach resonances in ultracold 39K. New J. Phys. 9, 223 (2007).

[49] Fetter, A. L. Walecka, J. D. Quantum Teory of Many-Particle Systems. (McGraw-Hill, Boston, 1971).

[50] L. Salasnich, V. Penna. Itinerant ferromagnetism of two-dimensional repulsive fermions with Rabi coupling. New J. Phys. 19, 043018 (2017).

[51] L. Dell'Anna, G. Mazzarella, L. Salasnich. Condensate fraction of a resonant Fermi gas with spin-orbit coupling in three and two dimensions. Phys. Rev. A 84, 033633 (2011).

[52] C. A. Regal, M. Greiner, and D. S. Jin. Observation of Resonance Condensation

of Fermionic Atom Pairs. Phys. Rev. Lett., 92, 2004.

[53] M. W. Zwierlein, C. A. Stan, C. H. Schunck, S. M. F. Raupach, A. J. Kerman, and W. Ketterle. Condensation of Pairs of Fermionic Atoms near a Feshbach Resonance. Phys. Rev. Lett., 92, 2004.